Supplementary Information

Deconvoluting XPS Spectra of La-containing Perovskites From First Principles

Ariel Whitten[1], Dezhou Guo[1], Elif Tezel[2], Reinhard Denecke[3] *, Eranda Nikolla[2,4] * and Jean-Sabin McEwen[1,5,6,7,8] *

[1]The Gene and Linda Voiland School of Chemical Engineering and Bioengineering, Washington State University, Pullman, WA, 99164, United States

[2] College of Engineering, Wayne State University, Detroit, Michigan, 48202, United States

[3] Wilhelm-Ostwald-Institute for Physical and Theoretical Chemistry, Leipzig University, Leipzig D-04103, Germany

[4] Department of Chemical Engineering and Material Science, University of Michigan, Ann Arbor, Michigan 48109, United States

[5] Department of Chemistry, Washington State University, Pullman, Washington, 99164, United States

[6] Department of Physics and Astronomy, Washington State University, Pullman, Washington, 99164, United States

[7] Department of Biological Systems Engineering, Washington State University, Pullman, Washington, 99164, United States

[8] Institute for Integrated Catalysis, Pacific Northwest National Laboratory, Richland, Washington 99352, United States

*Correspondence to: denecke@uni-leipzig.de (R. D.), erandan@umich.edu (E. N.) and js.mcewen@wsu.edu (J.-S. M.)

Procedure for volume equilibration

Equilibrium volumes for the $LaNiO_3$ and $LaCoO_3$ were described using a plane-wave cutoff energy of 500 eV. $LaNiO_3$ and $LaCoO_3$ have a trigonal unit cell with equal lattice constants (*a*=*b*=*c*), where we obtained the equilibrium volume by two steps: first, we selected one volume and relaxed the ionic position from the starting structure keeping the volume fixed with ISIF=2; then, we carried out a second ionic relaxation from the previous CONTCAR file to have an accurate description.

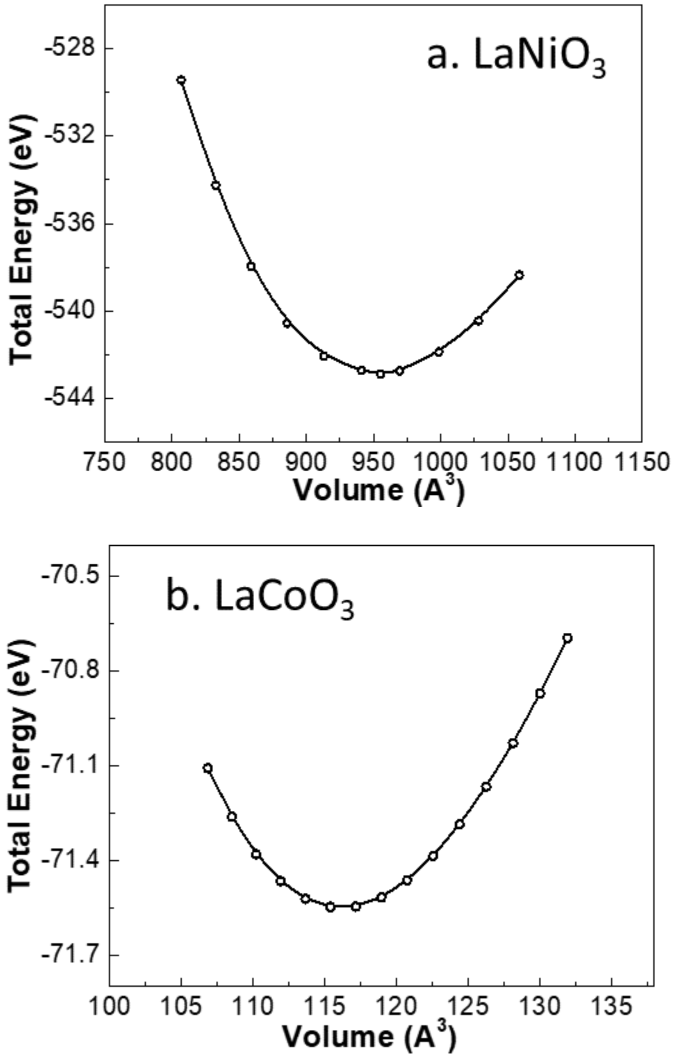

Figure S1: (a) Plot of total energy as function of volume for $LaNiO_3$. The spin polarized calculations were performed to properly capture the AFM ordering of the surface. The equilibrium volume of $LaNiO_3$ is 955.12 Å^3. (b) Plot of total energy as function of volume for $LaCoO_3$. Non-magnetic calculations were performed to describe this surface. The equilibrium volume of $LaCoO_3$ is 115.39 Å^3.

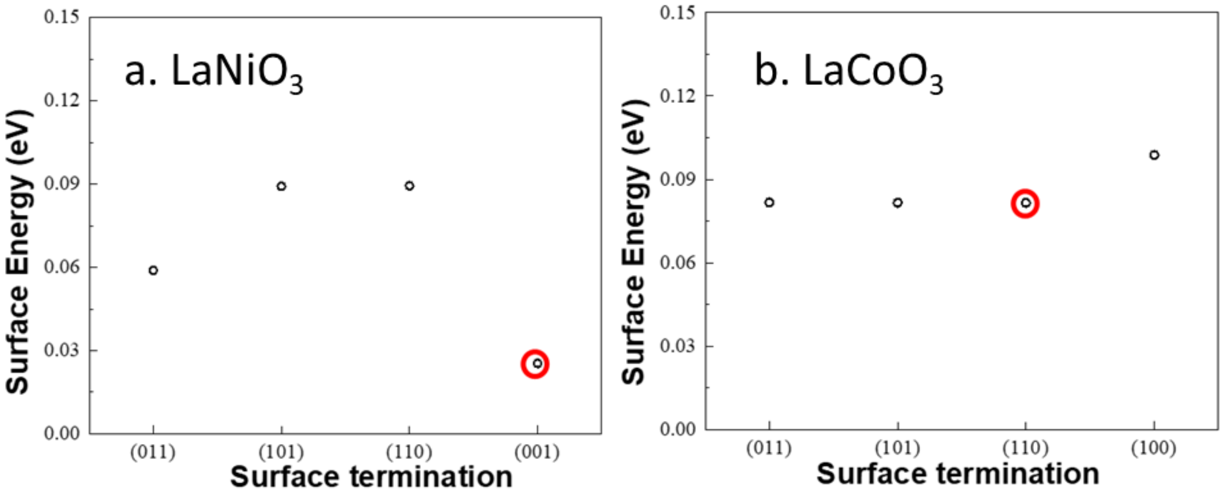

Figure S2: The surface energies of possible surface terminations for **a.** $LaNiO_3$ **b.** $LaCoO_3$ perovskite structures calculated based on Eq. 1 in the main manuscript. The red circles mark the energetically most favorable surface terminations. Reproduced from [1]. Copyright 2022 The Electrochemical Society ("ECS").

Equations S1 – S5 were used for calculating energy of adsorption for H (Equation S1), O (Equation S2), OH (Equation S3), H_2O (Equation S4) and CO_2 (Equation S5). B stands for either Ni or Co depending on surface being analyzed.

$$E_{\text{ads of H}} = E_{\text{H+LaBO}_3} - E_{\text{LaBO}_3} - 1/2E_{\text{H}_2} \quad \text{(Eq. S1)}$$

$$E_{\text{ads of O}} = E_{\text{O+LaBO}_3} - E_{\text{LaBO}_3} - 1/2E_{\text{O}_2} \quad \text{(Eq. S2)}$$

$$E_{\text{ads of OH}} = E_{\text{OH+LaBO}_3} - E_{\text{LaBO}_3} - (E_{\text{H}_2\text{O}} - 1/2E_{\text{H}_2}) \quad \text{(Eq. S3)}$$

$$E_{\text{ads of H}_2\text{O}} = E_{\text{H}_2\text{O+LaBO}_3} - E_{\text{LaBO}_3} - E_{\text{H}_2\text{O}} \quad \text{(Eq. S4)}$$

$$E_{\text{ads of CO}_2} = E_{\text{CO}_2\text{+LaBO}_3} - E_{\text{LaBO}_3} - E_{\text{CO}_2} \quad \text{(Eq. S5)}$$

Detailed Explanation of CLBES and CLBE Methods:

First, we consider both surfaces, $LaNiO_3$ and $LaCoO_3$ without adsorbates. After a geometry optimization of the surface cell, we perform single point calculations for each distinct, relaxed atom in the cell to calculate a final state energy with a core level electron removed from the orbital corresponding to the spectra of interest (i.e. for the O 1s spectra a 1s electron is removed from the oxygen atom being probed). Once all distinct, relaxed atoms have been sampled, we set the lowest energy final state approximation of these sampled atoms to the reference final state approximation energy, $E_{\mathrm{ref(n-1)}}$ (i.e., has a CLBES of 0 eV). We then use Equation 4 in the main text to solve for the CLBES of all other distinct, relaxed atoms in the cell resulting in the sampling of 24 atoms per surface spectra. The atom chosen for the reference energy is arbitrary as the differences between the CLBES will be consistent no matter the reference, but we specifically chose the lowest energy in the final state approximation to make most of our CLBESs positive for clarity. We use the same reference final state approximation energy, $E_{\mathrm{ref(n-1)}}$, used in the surface CLBES calculations to calculate the CLBES of atoms when an adsorbate is present on the surface using Equation 4 in the main text. The only major difference is we only sample three atoms near the adspecies and atoms within the adspecies that are represented in the spectra (i.e. all oxygen atoms present in a carbon dioxide molecule when investigating the O 1s spectra) in this step and not all distinct atoms within the surface to keep calculations tractable. For both the O 1s spectra produced, the surface spectra are composed of 24 oxygen atoms. The adspecies spectra use atoms sampled from the two most favorable configurations of adspecies pictured in Figure 2 and 4 for a total of 8 oxygen atoms (6 surface oxygen atoms and 2 adsorbed atoms) sampled for the H, O, OH and H_2O spectra and 10 oxygen atoms (6 surface oxygen atoms and 4 adsorbed atoms) sampled for the CO_2 spectra. The procedure for finding the reference atom for the C 1s spectra is different as no carbon species are present in perovskite lattice, therefore we must adsorb a carbon containing species to the surface for the reference final state approximation energy. Previous research used graphite sheets or benzene adsorbed to the surface as a reference value, but we opt to use a simple hydrocarbon on the surface, CH_4, to reduce the overall computational cost of creating this spectrum while also capturing the peak associated with adventitious carbon that are known to be present on the surface of perovskites at standard conditions. This procedure has been done before to calculate the binding energies of carbon-containing compounds on a Cu (111) surface[2].

Next, we separately combine the CLBESs associated with a clean surface and each surface with adspecies using Gaussian distributions to model the experimental XPS spectra. We broaden the CLBES using a peak width of 0.35 eV with equal weighting. Although the experimental resolution is 2 eV, we use a smaller value of 0.35 eV to distinguish the different contributions while also allowing us to see the two peaks observed in the experimental spectra that we could not observe if we only plotted single lines without broadening. Once the spectra have been generated, we must shift the CLBES values to the experimental binding energies because one cannot determine the absolute values of the core level binding energies using the Projected Augmented Wave method. However, one can obtain CLBESs. To calibrate the core level binding energy values, we obtain $E_{\text{experimental}}$ by shifting the apex of the lower energy peak of the theoretical spectra from the clean surface so that it aligns with the lower energy experimental peak associated with surface species. We add the shift to all CLBES to get the corresponding CLBE for all surface atoms and adspecies. This allows us to investigate the contributions of the surface and adsorbed species in comparison to the experimental spectra. Note: Some CLBES of atoms will be calculated multiple times to understand the difference between atoms without adsorbates within a clean surface and the same atoms with adsorbates. We show the fully deconvoluted spectra for oxygen O 1*s* spectra on the LaNiO$_3$ surface in Figure S3.

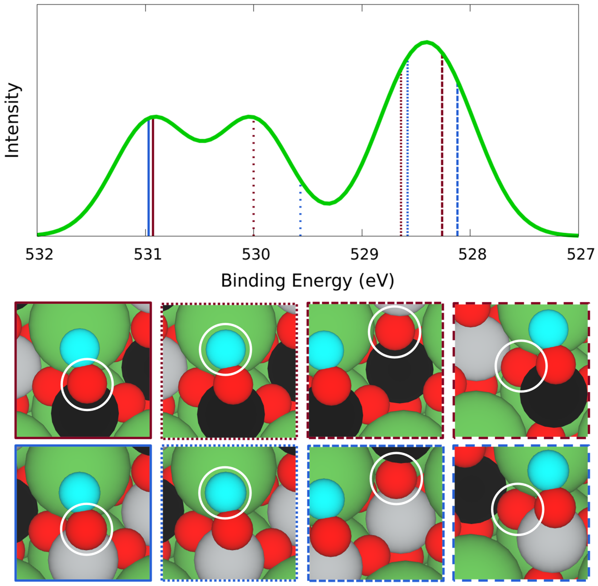

Figure S3: An example of a fully deconvoluted O 1*s* spectra for oxygen on the LaNiO$_3$ surface. Below the graph are images of species contributing to each of the peaks in the presence of adsorbed atoms/molecules. The border color and line type correspond to the energies marked on the theoretical XPS graph. Spin up and spin down Ni are shown in black and grey, respectively. The corresponding O species for which the XPS is simulated are circled in white. The blue and red spheres represent an oxygen adspecies and a lattice oxygen, respectively.

As seen in the graph, the several contributions of like atoms on spin up and spin down surfaces are very similar, which is the case for all adspecies. We reduced the number of labelled adspecies in the text for clarity and conciseness.

Note: For the theoretical spectra for $LaCoO_3$ shown in Figure 7, we sampled half of the relaxed surface atoms and all the adsorbates. The rationale for this reduced sampling is that there are many atoms with the same CLBEs in the surface spectra as shown in Table S7. The CLBEs of atoms within the surface spectra are only affected by depth and the local coordination of the surface atom. The largest difference in energy between atoms in the same depth and local coordination is 0.01 eV which is close to DFT error. When obtaining the CLBESs of lattice oxygen species surrounding an adsorbate, we performed two calculations: One in the presence of adsorbates and one without adsorbates. In the calculations of the clean surface (without adsorbates), some core level binding energies of the lattice oxygen sampled were not computed. In those cases, the clean surface equivalent was used to find their CLBES during the computation of the surface spectra. Indeed, we can still compare the CLBES values to an equivalent atom in the computed surface spectra because most likely they have the same CLBES as the atom sampled in the adsorbate calculation.

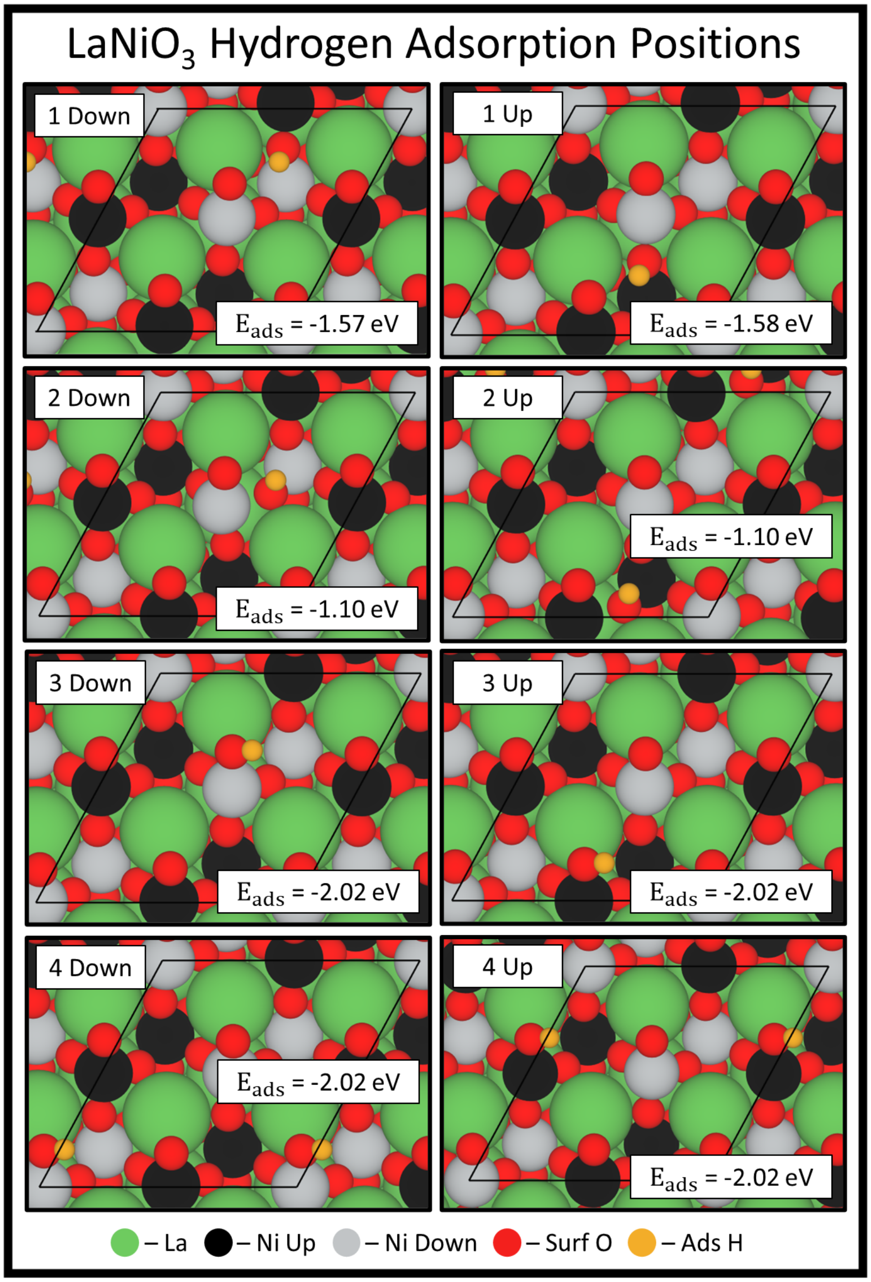

Figure S4: The optimized adsorption site positions for hydrogen on NiO-terminated LaNiO$_3$ (001). The adsorption energy (in eV) is labelled within the box. Spin up and spin down Ni are shown in black and grey respectively.

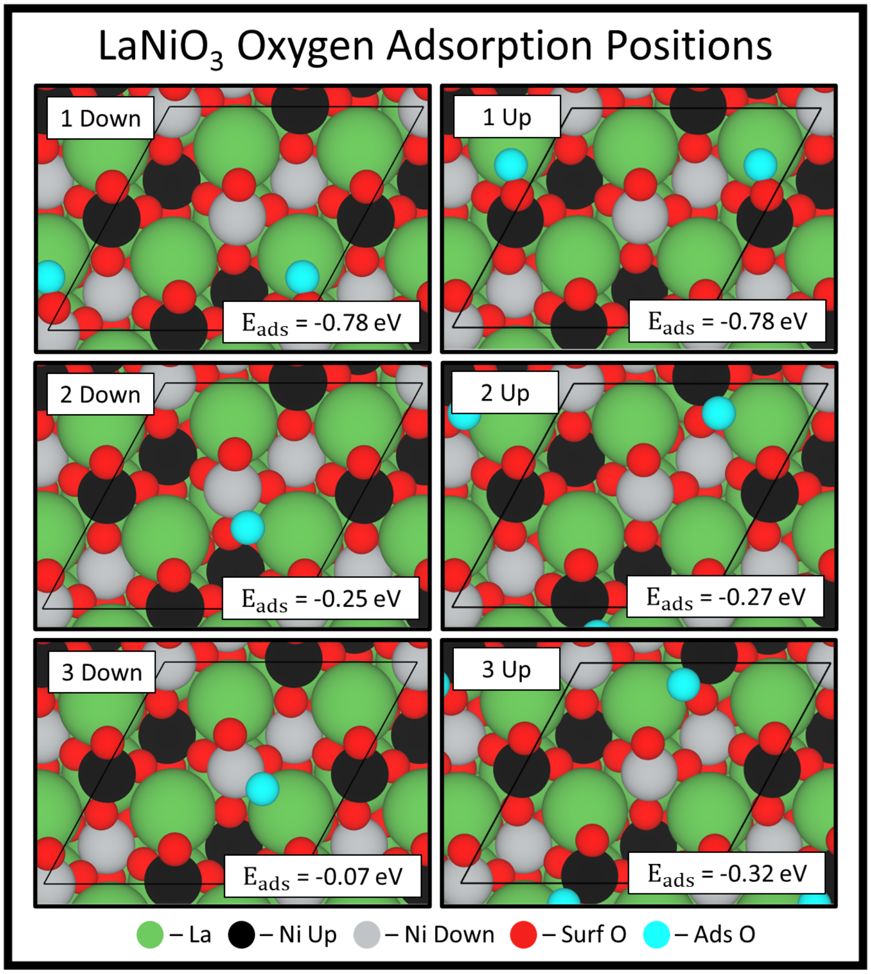

Figure S5: The optimized adsorption site positions for oxygen on NiO-terminated LaNiO$_3$ (001). The adsorption energy (in eV) is labelled within the box. Spin up and spin down Ni are shown in black and grey respectively.

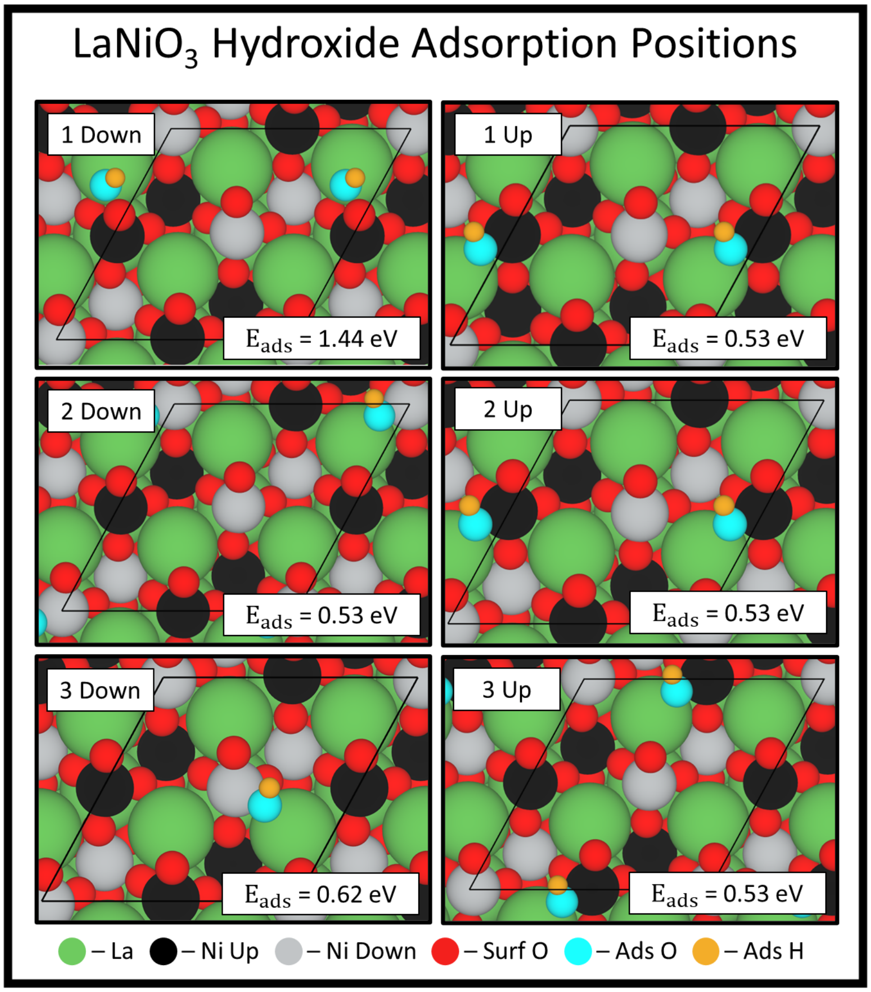

Figure S6: The optimized adsorption site positions for hydroxide on NiO-terminated $LaNiO_3$ (001). The adsorption energy (in eV) is labelled within the box. Spin up and spin down Ni are shown in black and grey respectively.

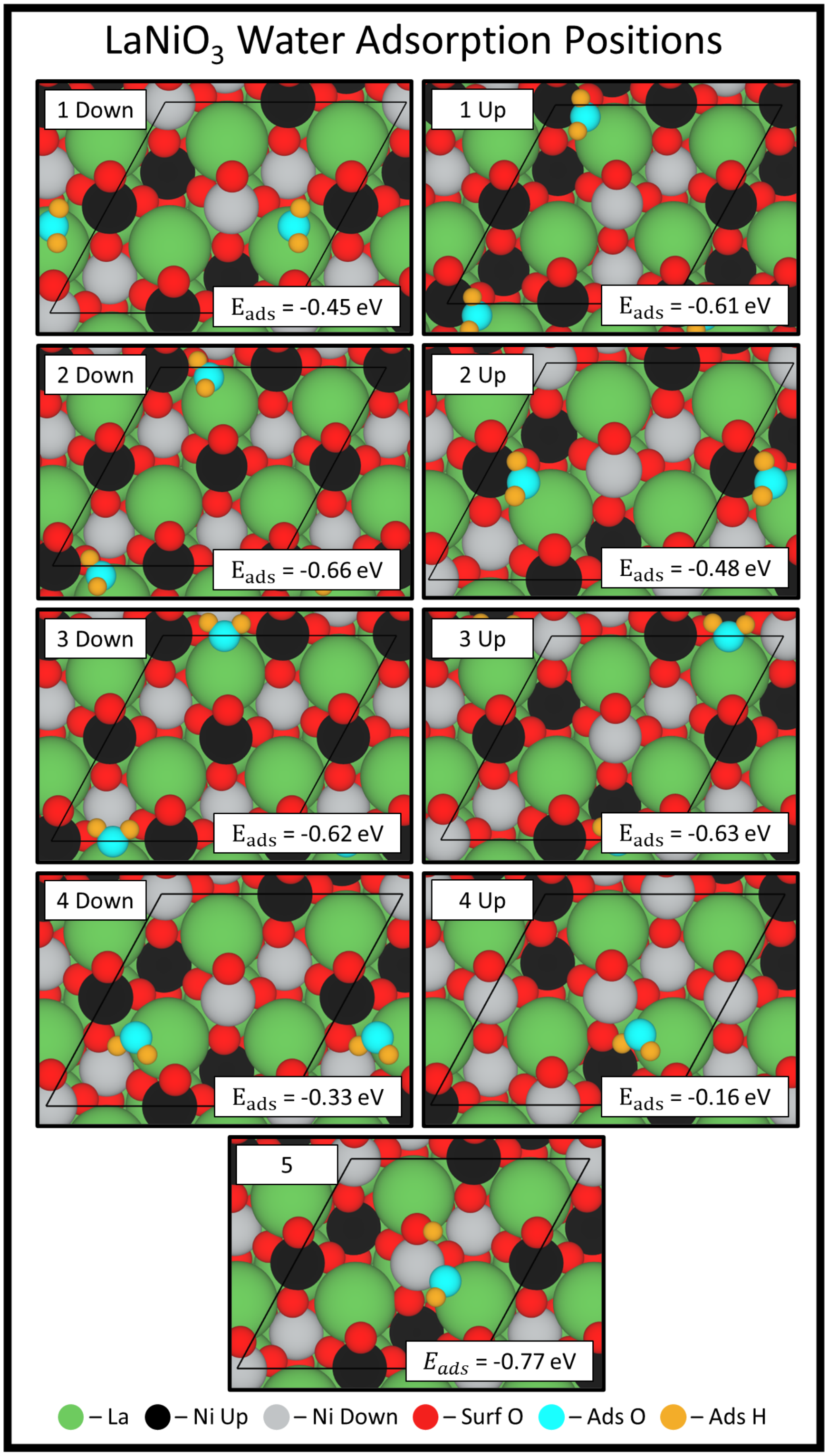

Figure S7: The optimized adsorption site positions for water on NiO-terminated $LaNiO_3$ (001). The adsorption energy (in eV) is labelled within the box. Spin up and spin down Ni are shown in black and grey respectively.

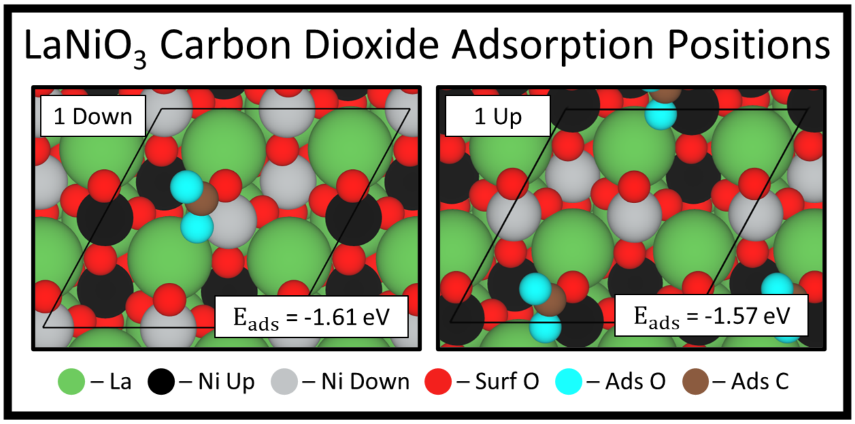

Figure S8: The optimized adsorption site positions for carbon dioxide on NiO-terminated LaNiO$_3$ (001). The adsorption energy (in eV) is labelled within the box. Spin up and spin down Ni are shown in black and grey respectively.

Table S1: Bond length, bond angle and depth information for each adsorbate on the LaNiO$_3$ surface.

H		
Configuration	H*-O (Å)	Depth (Å)
1 Down	0.98	-0.43
2 Down	0.98	-0.95
3 Down	0.98	0.57
4 Down	0.98	0.53
1 Up	0.98	-0.44
2 Up	0.98	-0.98
3 Up	0.97	0.57
4 Up	0.98	0.58

O			
Configuration	O*-La (Å)	O*-Ni (Å)	O*-O (Å)
1 Down	2.60	2.80	1.32
2 Down	2.77	1.91	1.44
3 Down	2.47	1.72	2.7
1 Up	2.60	2.80	1.32
2 Up	2.72	1.90	1.44
3 Up	2.62	1.90	1.44

OH		
Configuration	O*-La (Å)	O*-Ni (Å)
1 Down	2.76	2.85
2 Down	2.45	1.89
3 Down	2.49	1.89
1 Up	2.45	1.91
2 Up	2.45	1.90
3 Up	2.47	1.89

H_2O				
Configuration	O*-La (Å)	O*-Ni (Å)	O*-H* (Å)	O*-H* (Å)
1 Down	2.68	3.26	0.97	0.97
2 Down	2.74	2.87	0.99	0.97
3 Down	2.81	3.19	0.98	0.98
4 Down	2.84	2.91	0.98	0.97
1 Up	3.03	2.19	0.98	0.99
2 Up	2.95	2.26	0.98	1.00
3 Up	2.81	3.21	0.98	0.99
4 Up	2.85	2.85	0.98	0.98

CO_2						
Configuration	O*-La (Å)	O*-Ni (Å)	O*-C*-1 (Å)	O*-C*-2 (Å)	C*-O (Å)	O*-C*-O* (º)
1 Down	2.68	1.92	1.35	1.22	1.37	127.01
1 Up	2.71	1.91	1.35	1.21	1.36	126.81

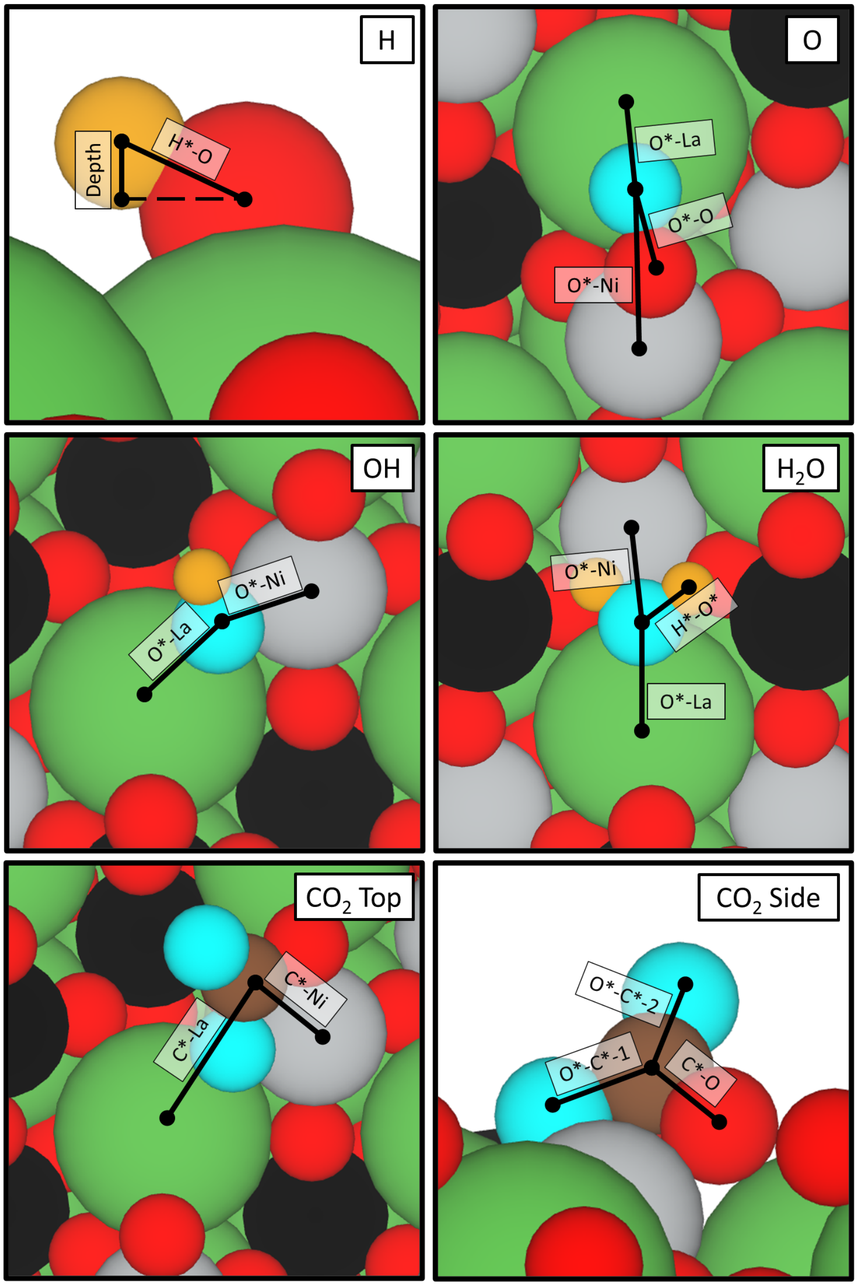

Figure S9: A key for Table S1 about bond length and depth information for each adsorbate on the $LaNiO_3$ surface. The sphere color legend is the same as Figures S4 to S8.

Table S2: Magnetization (in units of μ_B) of surface nickel atoms in $LaNiO_3$ surface for all adspecies in the most favorable configuration for both the spin up and spin down compared to the bare surface. Negative values are marked in white or lighter grey and positive values are marked in darker grey. The corresponding configurations are shown in Figure S3 to S7. The figure above shows the positions of atoms in the surface that can be compared across cases.

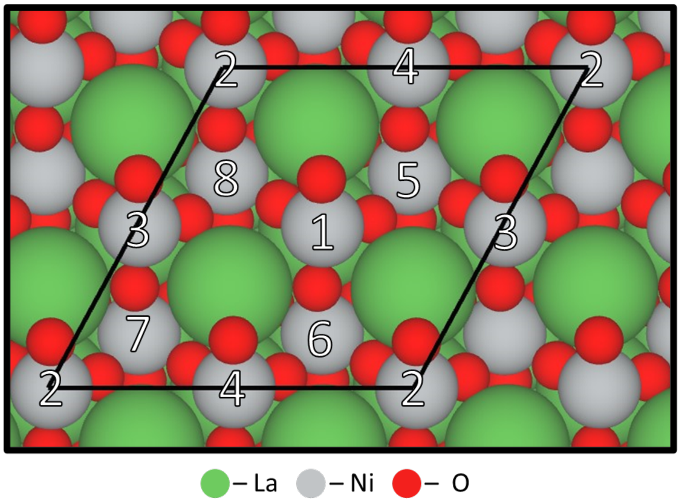

Atom Identifiers		Magnetization Value (in μ_B)										
		Surface	H		O		OH		H_2O		CO_2	
Ni #	Z-position (Å)		3 Down	3 Up	1 Down	1 Up	2 Down	1 Up	2 Down	3 Up	1 Down	1 Up
1	12.57	-0.789	-0.74	-0.84	-0.912	-0.84	-0.979	-0.935	0.77	-0.875	-0.827	-0.832
2	12.57	-0.733	-0.954	-0.809	-0.735	-0.809	-0.797	-1.375	0.739	-0.83	0.534	0.453
3	12.56	0.96	0.81	0.971	0.889	0.971	0.881	0.776	0.737	0.885	-0.835	-0.835
4	12.55	0.693	0.836	0.736	0.805	0.736	0.942	0.933	0.722	0.812	0.832	-0.833
5	10.61	-0.723	-0.835	-0.779	-0.777	-0.779	-0.77	-0.775	-0.861	-0.805	-0.841	-0.772
6	10.60	0.763	0.773	0.834	0.869	0.834	0.768	0.679	-0.82	0.823	0.825	0.937
7	10.60	0.788	-0.792	-0.859	-0.798	-0.859	-0.773	0.139	-0.825	-0.801	0.059	-1.339
8	10.58	0.76	0.858	0.79	0.773	0.79	0.736	0.716	-0.787	0.777	-0.74	0.734

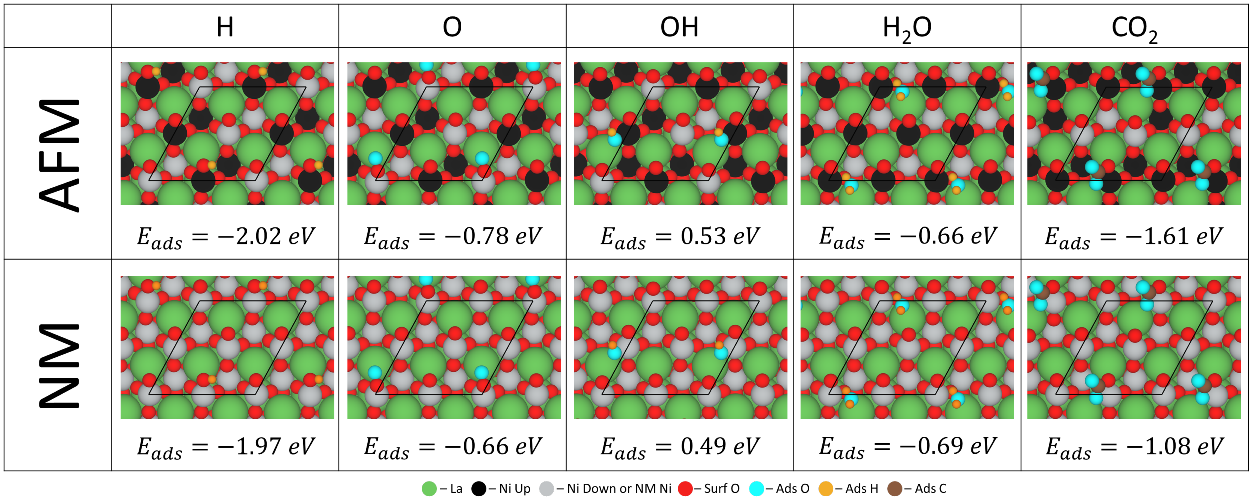

Figure S10: A comparison between adsorbate adsorption energies under AFM and NM ordering on the surface of $LaNiO_3$. The case for each adsorbate was chosen as the most favorable adsorption position under AFM effects.

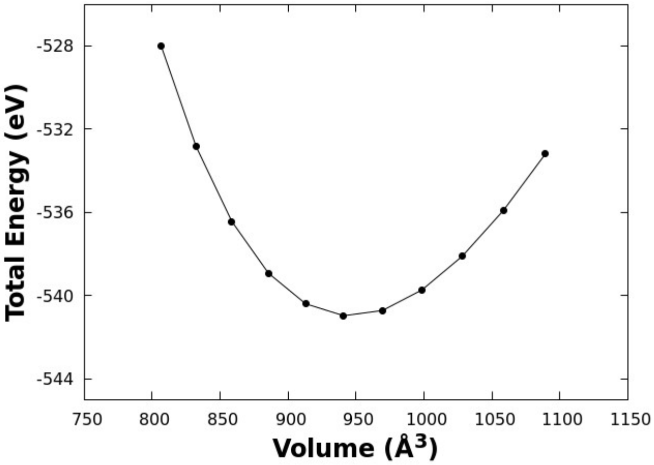

Figure S11: Plot of total energy as function of volume for NM $LaNiO_3$. The equilibrium volume of NM $LaNiO_3$ is 940.94 Å^3.

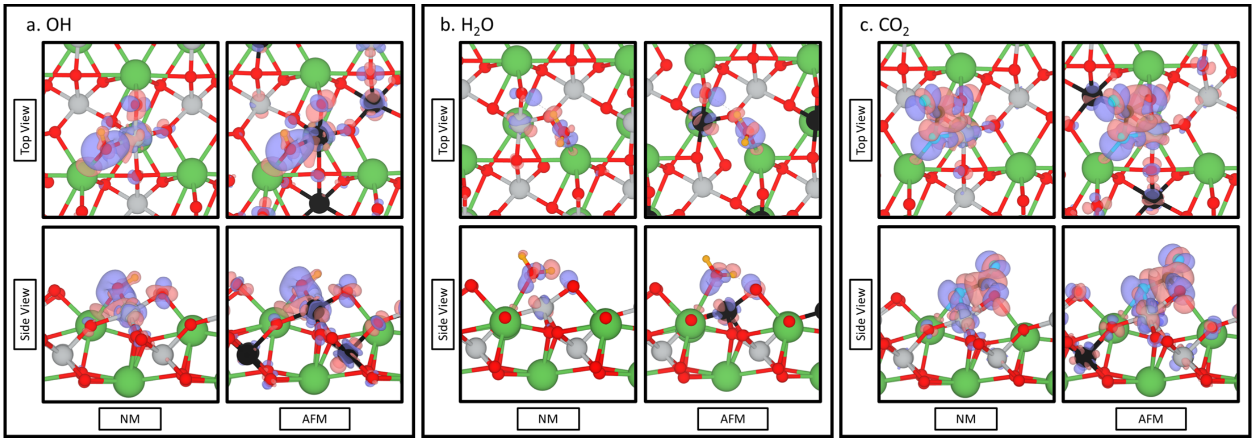

Figure S12: Charge transfer calculations for most favorable configurations of a. OH, b. H_2O and c. bidentate CO_2 on a $LaNiO_3$ Isosurface used is 0.005 electrons/Bohr^3. Red indicates charge gain and blue indicates charge loss. This was done on a 2-layer slice of relaxed atoms due to inability to produce readable CHGCAR files when AFM ordering was applied with a 6-layer surface.

Table S3: Bader charge analysis for NM $LaNiO_3$ Surface. The adsorbed species are listed as well as the surface species bonded to the adsorbed molecule. The difference is computed by subtracting (charge before adsorption) from (charge after adsorption).

Adsorbate	Contribution	Atom	Charge before adsorption (*e*)	Charge after adsorption (*e*)	Difference (*e*)
OH	Adsorbed	O	-1.15	-1.06	-0.09
		H	0.57	0.61	-0.04
	Surface	La	2.09	2.14	-0.05
		Ni	1.11	1.24	-0.13
H_2O	Adsorbed	O	-1.15	-1.24	0.09
		H1	0.57	0.63	-0.06
		H2	0.58	0.63	-0.05
	Surface	La	2.09	2.13	-0.04
CO_2	Adsorbed	C	2.06	2.11	-0.05
		O1	-1.02	-1.09	0.07
		O2	-1.05	-1.04	-0.01
	Surface	La	2.09	2.14	-0.05
		Ni	1.10	1.14	-0.04
		O	-0.89	-1.05	0.16

Table S4: Bader charge analysis for AFM $LaNiO_3$ Surface. The adsorbed species are listed as well as the surface species bonded to the adsorbed molecule. The difference is computed by subtracting (charge before adsorption) from (charge after adsorption).

Adsorbate	Contribution	Atom	Charge before adsorption (*e*)	Charge after adsorption (*e*)	Difference (*e*)
OH	Adsorbed	O	-1.15	-1.07	-0.08
		H	0.57	0.57	0.00
	Surface	La	2.11	2.16	-0.05
		Ni	1.17	1.24	-0.07
H2O	Adsorbed	O	-1.15	-1.27	0.12
		H1	0.57	0.65	-0.08
		H2	0.58	0.64	-0.06
	Surface	La	2.09	2.15	-0.06
CO2	Adsorbed	C	2.06	2.11	-0.05
		O1	-1.02	-1.05	0.03
		O2	-1.05	-1.08	0.03
	Surface	La	2.13	2.15	-0.02
		Ni	1.07	1.15	-0.08
		O	-0.90	-1.05	0.15

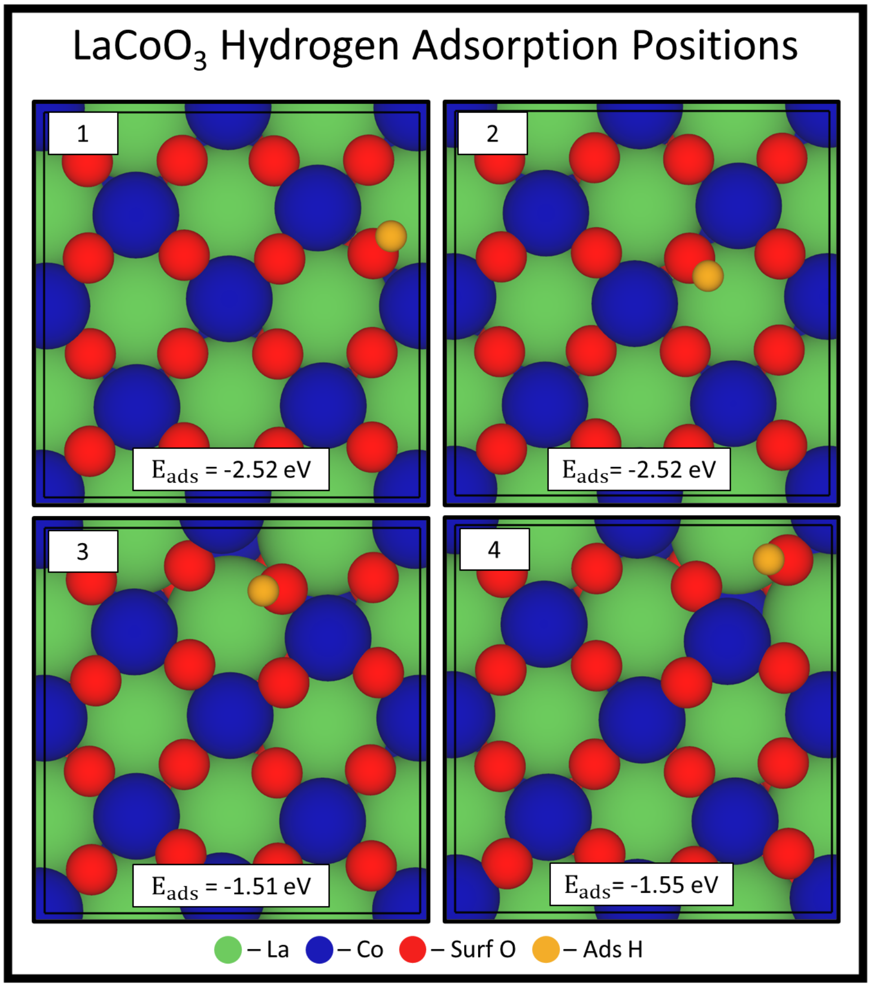

Figure S13: The optimized adsorption site positions for hydrogen on CoO-terminated $LaCoO_3$ (110). The adsorption energy (in eV) is listed in the bottom of each panel.

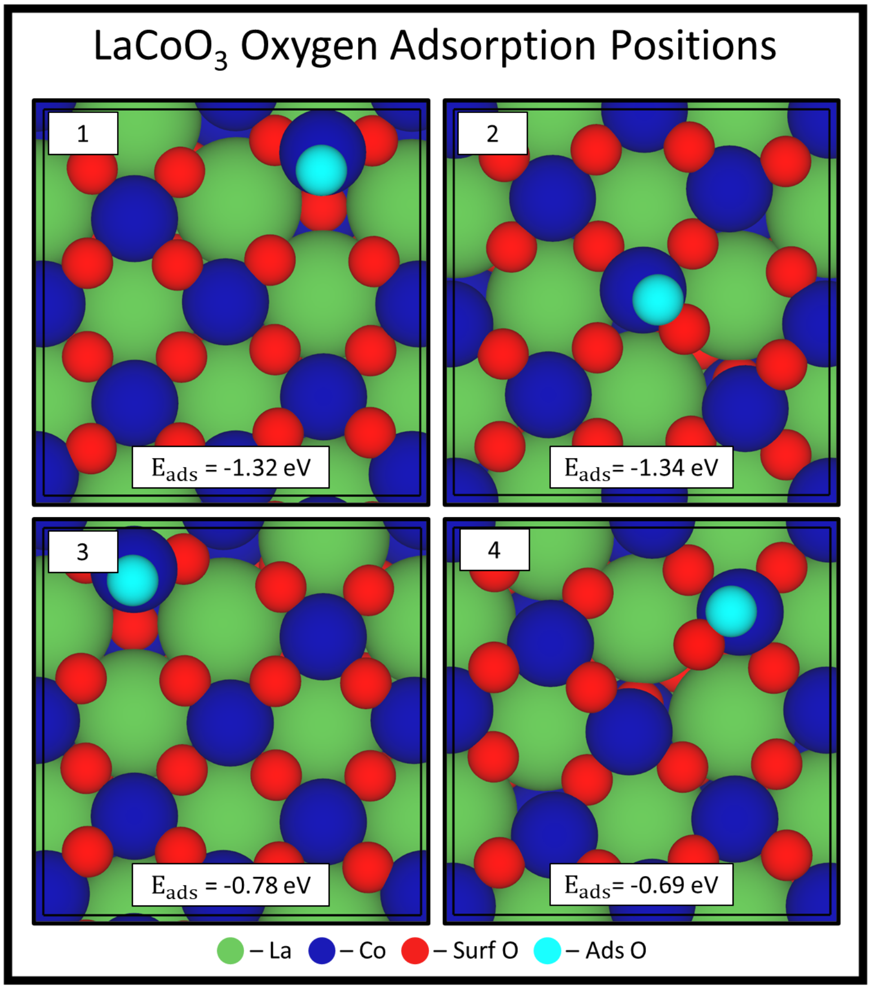

Figure S14: The optimized adsorption site positions for oxygen on CoO-terminated $LaCoO_3$ (110). The adsorption energy (in eV) is listed in the bottom of each panel.

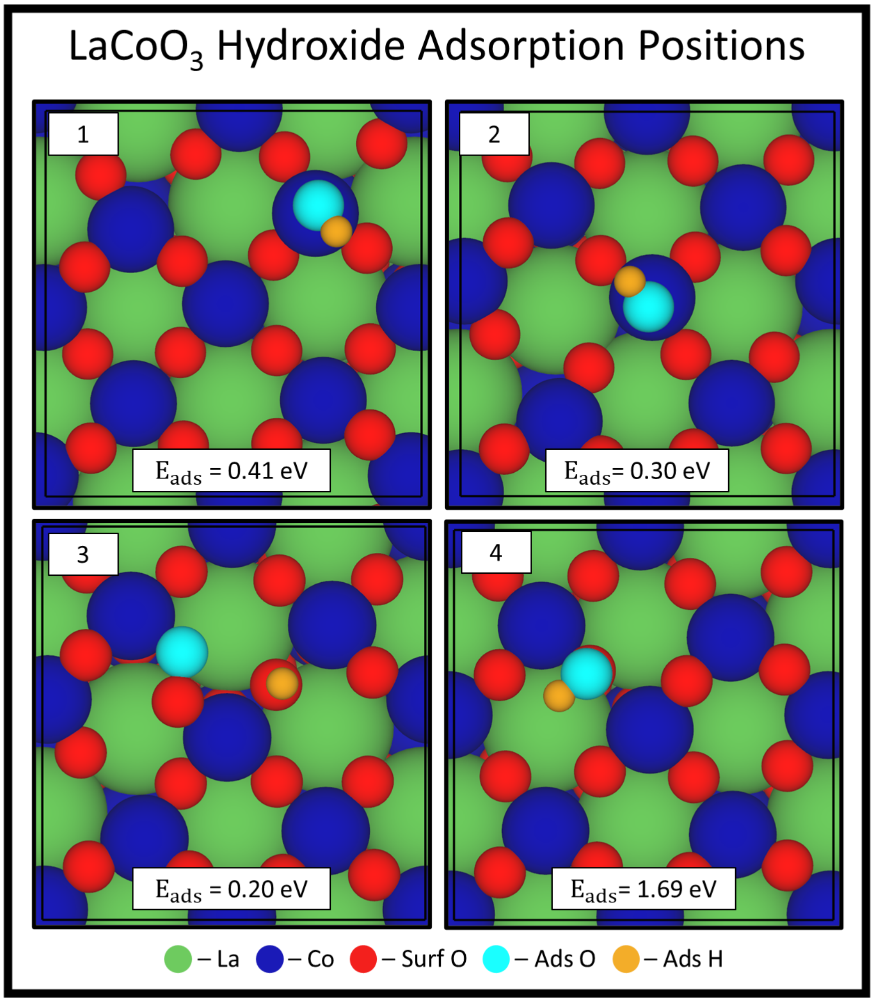

Figure S15: The optimized adsorption site positions for hydroxide on CoO-terminated LaCoO$_3$ (110). The adsorption energy (in eV) is listed in the bottom of each panel.

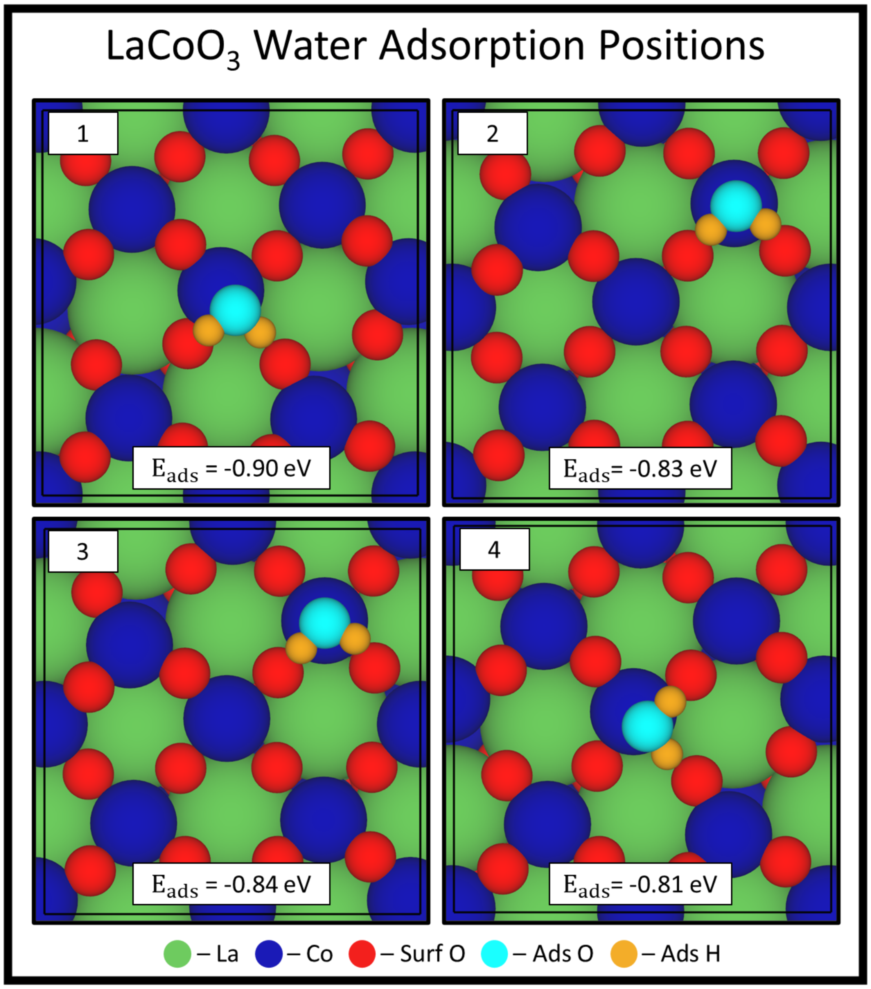

Figure S16: The optimized adsorption site positions for water on CoO-terminated $LaCoO_3$ (110). The adsorption energy (in eV) is listed in the bottom of each panel.

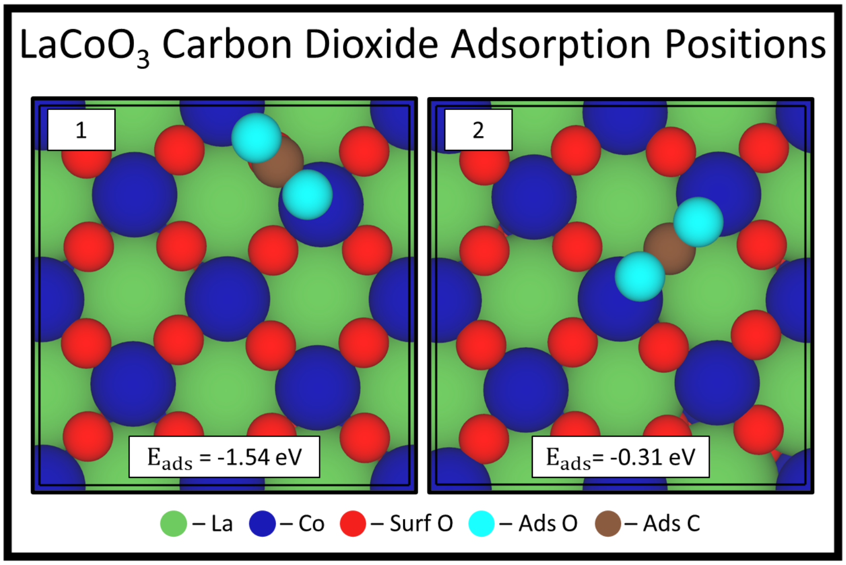

Figure S17: The optimized adsorption site positions for carbon dioxide on CoO-terminated $LaCoO_3$ (110). The adsorption energy (in eV) is listed in the bottom of each panel.

Table S5: Bond length, bond angle and depth information for each adsorbate on the $LaCoO_3$ surface.

H			
Configuration	H*-O (Å)	O-Co (Å)	O-Co (Å)
1	0.98	2.10	2.11
2	0.98	2.10	2.11
3	0.97	1.93	2.85
4	0.97	1.92	2.90

O				
Configuration	O*-La (Å)	O*-Co (Å)	O*-O (Å)	Co Lift (Å)
1	4.99	1.59	2.95	1.31
2	5.00	1.59	2.95	1.34
3	4.32	1.81	1.35	0.26
4	4.65	1.75	1.35	0.47

OH		
Configuration	O*-La (Å)	O*-Co (Å)
1	4.67	1.76
2	4.65	1.76
3	2.78	1.87
4	3.91	2.60

H_2O				
Configuration	O*-La (Å)	O*-Co (Å)	O*-H* (Å)	O*-H* (Å)
1	4.42	2.04	0.98	1.00
2	4.43	1.98	0.99	0.98
3	4.47	1.98	0.99	0.98
4	4.32	2.01	0.98	1.00

CO_2						
Configuration	O*-Co (Å)	O*-Co (Å)	O*-C*-1 (Å)	O*-C*-2 (Å)	C*-O (Å)	O*-C*-O* (º)
1	2.92	1.90	1.31	1.23	1.40	130.23
2	2.18	2.02	1.26	1.28	1.37	132.56

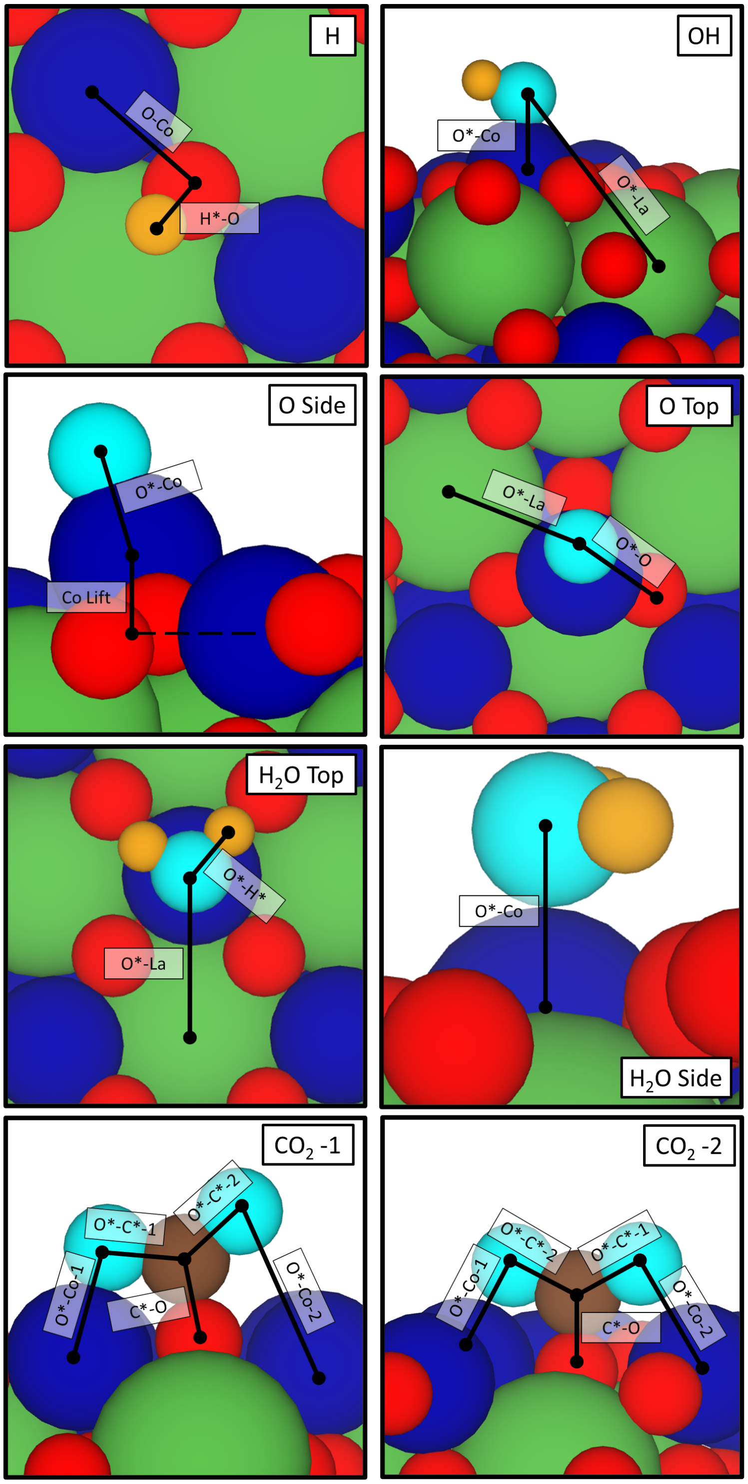

Figure S18: A key for Table S5 about bond length and depth information for each adsorbate on the $LaCoO_3$ surface. The sphere color legend is the same as Figures S13 to S17.

Table S6: Bader charge analysis for $LaNiO_3$ Surface. The adsorbed species are listed as well as the surface species bonded to the adsorbed molecule.

Adsorbate	Contribution	Atom	Charge before adsorption (*e*)	Charge after adsorption (*e*)	Difference (*e*)
OH	Adsorbed	O	-1.15	-1.07	-0.08
		H	0.57	0.57	0.00
	Surface	La	2.11	2.16	-0.05
		Ni	1.15	1.23	-0.08
H_2O	Adsorbed	O	-1.15	-1.25	0.10
		H1	0.57	0.62	-0.05
		H2	0.58	0.64	-0.06
	Surface	La	2.11	2.15	-0.04
CO_2	Adsorbed	C	2.06	2.11	-0.05
		O1	-1.02	-1.05	0.03
		O2	-1.05	-1.08	0.03
	Surface	La	2.11	2.11	0.00
		Ni	1.15	1.14	0.01
		O	-0.83	-1.04	0.21

Table S7: Bader charge analysis for $LaCoO_3$ Surface. The adsorbed species are listed as well as the surface species bonded to the adsorbed molecule. O1 is the oxygen closer to the surface in the bidentate configuration and O2 is further from the surface.

Adsorbate	Contribution	Atom	Charge before adsorption (*e*)	Charge after adsorption (*e*)	Difference (*e*)
OH	Adsorbed	O	-1.15	-0.88	-0.27
		H	0.57	0.56	0.01
	Surface	Co	2.30	2.36	-0.06
H_2O	Adsorbed	O	-1.15	-1.13	-0.02
		H1	0.57	0.64	-0.07
		H2	0.58	0.62	-0.04
	Surface	Co	2.30	2.29	0.01
CO_2 Bidentate	Adsorbed	C	2.06	2.12	-0.06
		O1	-1.02	-0.95	-0.07
		O2	-1.05	-1.11	0.06
	Surface	Co	2.30	2.33	-0.03
		O	-0.87	-0.84	-0.03
CO_2 Monodentate	Adsorbed	C	2.06	2.16	-0.10
		O1	-1.02	-1.00	-0.02
		O2	-1.05	-1.04	-0.01
	Surface	Co1	2.30	2.34	-0.04
		Co2	2.30	2.31	-0.01
		O	-1.06	-1.14	0.08

Detailed Description of CLBEs for $LaNiO_3$

H Adsorption: The addition of the H also increased the CLBEs of surrounding bulk oxygens by 0.30 ± 0.10 eV (Figure 6 H-2 and H-3).

O Adsorption: The adsorption of O on the surface increased the CLBEs of the closely situated surface O by 3.62 ± 0.01 eV to 530.9 ± 0.02 eV (Figure 6 O-3). The bulk atoms under the influence of O adspecies only have an increase in CLBEs of 0.13 ± 0.06 eV (Figure 6 O-2), a much smaller shift than the undercoordinated surface oxygens.

OH Adsorption: Adsorbing OH on the surface led to a decrease in CLBEs of the lattice O by 0.39 ± 0.40 eV (Figure 6 OH-2 and OH-3).

H_2O Adsorption: The CLBEs of surrounding surface O shift by 0.19 ± 0.01 eV (Figure 6 H_2O-3) in the presence of water and the bulk oxygens' CLBE shift slightly by 0.09 ± 0.06 eV (Figure 6 H_2O-2).

CO_2 Adsorption: The adsorbed O closer to the surface had an average CLBE of 530.15 ± 0.06 eV (Figure 6 CO_2-1) and the O facing the vacuum had an average CLBE of 529.74 ± 0.09 eV (Figure 6 CO_2-3). The surface O for which the CO_2 molecule adsorbs onto significantly increased in CLBEs with an average value of 530.12 ± 0.11 eV, a 2.86 ± 0.09 eV shift from the clean surface value (not marked in Figure 6 but shown in red in CO_2-1 and CO_2-3). The surrounding oxygen atoms predominately increased in CLBE by 0.11 ± 0.10 eV (Figure 6 CO_2-2).

Table S8: CLBESs contributions to each theoretical spectra shown in Figure 6 for $LaNiO_3$. These values have been convoluted using Gaussians to create theoretical spectra. The atom labels for the surface without adsorbates refer to those of the associated .cif file (LaNiO3_structure.cif).

Surface			
Atom	Z-Pos (Å)	CLBE (eV)	CLBES (eV)
O1	13.57	527.25	0.00
O2	13.60	527.28	0.03
O3	13.60	527.29	0.04
O4	13.59	527.27	0.02
O5	12.09	528.00	0.75
O6	12.07	527.94	0.69
O7	12.05	527.94	0.69
O8	12.04	527.98	0.73
O9	11.49	528.43	1.18
O10	11.48	528.44	1.19
O11	11.47	528.43	1.18
O12	11.47	528.36	1.11
O13	11.35	528.46	1.21
O14	11.33	528.46	1.21
O15	11.32	528.44	1.19
O16	11.32	528.47	1.22
O17	9.73	528.28	1.03
O18	9.73	528.28	1.03
O19	9.73	528.27	1.02
O20	9.72	528.28	1.03
O21	9.40	528.20	0.95
O22	9.39	528.20	0.95
O23	9.38	528.21	0.96
O24	9.38	528.18	0.93

H			
Atom	Site	CLBE (eV)	CLBES (eV)
O1	3 Up	530.03	2.78
O11	3 Up	528.73	1.48
O5	3 Up	528.24	0.99
O4	4 Down	530.27	3.02
O9	4 Down	528.90	1.65
O8	4 Down	528.17	0.92

O			
Atom	Site	CLBE (eV)	CLBES (eV)
O3	1 Up	530.88	3.63
O6	1 Up	528.21	0.96
O16	1 Up	528.59	1.34
Oads	1 Up	529.95	2.70
O4	1 Down	530.92	3.67
O8	1 Down	528.07	0.82
O13	1 Down	528.53	1.28
Oads	1 Down	529.97	2.72

OH			
Atom	Site	CLBE (eV)	CLBES (eV)
O3	1 Up	527.23	-0.02
O8	1 Up	528.07	0.82
O16	1 Up	528.19	0.94
Oads	1 Up	529.57	2.32
O4	2 Down	526.93	-0.32
O13	2 Down	527.30	0.05
O6	2 Down	527.86	0.61
Oads	2 Down	529.55	2.30

H_2O			
Atom	Site	CLBE (eV)	CLBES (eV)
O2	2 Up	527.44	0.19
O9	2 Up	528.43	1.18
O6	2 Up	528.03	0.78
Oads	2 Up	532.38	5.13
O2	4 Down	527.43	0.18
O9	4 Down	528.60	1.35
O6	4 Down	528.04	0.79
Oads	4 Down	531.60	4.35

CO_2			
Atom	Site	CLBE (eV)	CLBES (eV)
O1	1 Up	530.02	2.77
O15	1 Up	528.55	1.30
O7	1 Up	528.10	0.85
Oads1	1 Up	530.09	2.84
Oads2	1 Up	529.66	2.41
O5	1 Down	528.22	0.97
O14	1 Down	528.40	1.15
O2	1 Down	530.23	2.98
Oads1	1 Down	530.21	2.96
Oads2	1 Down	529.83	2.58

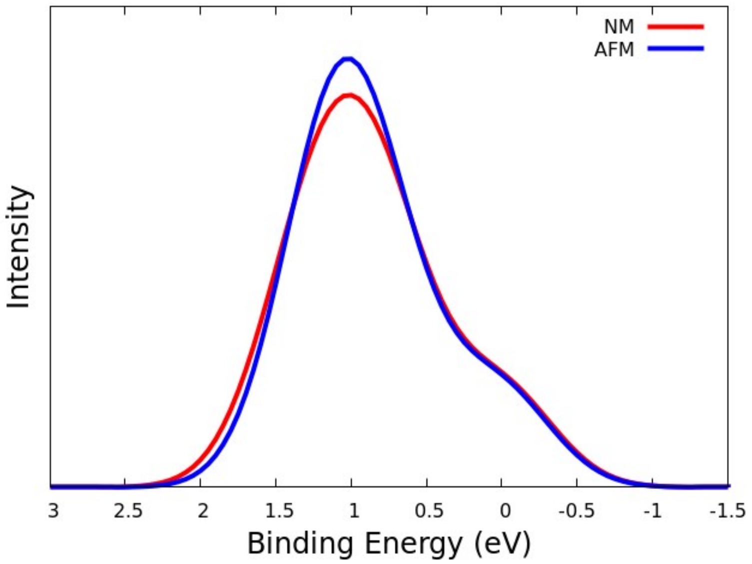

Figure S19: Comparison between O 1*s* spectra under AFM and NM ordering for $LaNiO_3$. Spectra was produced using the same surface and is composed of the same atoms within the model perovskite lattice.

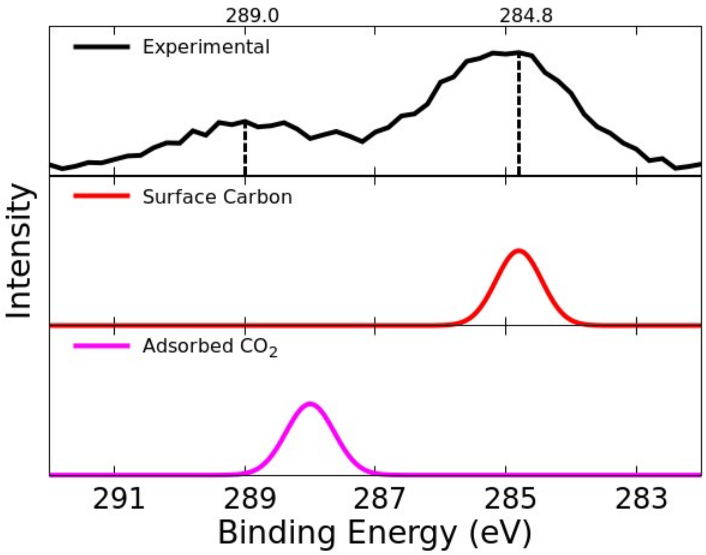

Figure S20: Experimental XPS C 1*s* $LaNiO_3$ surface data plotted with two peaks one at 284.8 eV and one at 289.0 eV.

Detailed Description of CLBEs for $LaCoO_3$

H Adsorption: The surrounding oxygens also shifted in CLBEs with an average shift of 1.08 ± 0.07 eV (Figure 7 H-2 and H-3).

O Adsorption: When the Co lifts from the surface, the surface O that the Co atoms lifts away from decreases by 0.74 ± 0.03 eV (Figure 7 O-3).

OH Adsorption: The surrounding atoms typically increase in CLBE by an average of 0.41 ± 0.06 eV (Figure 7 OH-2) but the surface O below the adsorbed H decreases by 0.25 ± 0.03 eV (Figure 7 OH-3).

H_2O Adsorption: The trends of the surrounding atoms are not clear. For adsorption Site 3 in Figure 4, the CLBE of the O below the adsorbed H decreased by 0.46 ± 0.03 eV (Figure 7 H_2O-3) and the CLBE of another nearby surface atom (similar to Figure 7 H_2O-2) increased by 0.38 eV. In adsorption Site 1 in Figure 4 for H_2O, one of the O below the adsorbed H had its CLBE increase by 0.04 eV and the O below the other H decreased by -0.03 eV. The CLBE of the third O (Figure 7 H_2O-2) decreased by 0.14 eV. The adsorption positions of the water on the surface are different in these sites and this may account for the differences in the CLBEs of both the adsorbed and surface O.

CO_2 Adsorption: For the bidentate adsorption, the surface O beneath the CO_2 has the largest shift of 3.28 eV and the other surface oxygens also increase in energy by 0.54 eV and 1.49 eV (both oxygens in a similar position pictured in Figure 7 CO_2-2). For the monodentate adsorption, the CLBE of the surface O beneath the C atom increases by 2.65 eV thus having the largest shift. The CLBE of both the other surface oxygen decrease by 0.41 eV and 0.09 eV (Figure 7 CO_2-2).

Table S9: CLBESs contributions to each theoretical spectra shown in Figure 7 for $LaCoO_3$. These values have been convoluted using Gaussians to obtain the simulated spectra. The stars denote the oxygen that were not sampled in the original surface calculations and have been replaced with an equivalent atom as explained in the Detailed Explanation of CLBES and CLBE Methods. The atom labels for the surface without adsorbates refer to those of the associated .cif file (LaCoO3_structure.cif).

Surface			
Atom	Z-Position (Å)	CLBE (eV)	CLBES (eV)
O1	13.97	528.26	0.34
O2	13.97	528.26	0.34
O3	13.97	528.26	0.34
O4	13.97	528.26	0.34
O5	13.45	527.92	0.00
O6	13.45	527.92	0.00
O7	13.45	527.92	0.00
O8	13.45	527.92	0.00
O9	11.78	528.95	1.03
O10	11.78	528.95	1.03
O11	11.78	528.95	1.03
O12	11.78	528.95	1.03
O13	10.17	528.63	0.71
O14	10.17	528.63	0.71
O15	10.17	528.63	0.71
O16	10.17	528.63	0.71
O17	9.57	528.57	0.65
O18	9.57	528.57	0.65
O19	9.57	528.57	0.65
O20	9.57	528.57	0.65
O21	7.95	528.72	0.80
O22	7.95	528.72	0.80
O23	7.95	528.72	0.80
O24	7.95	528.71	0.79

H			
Atom	Site	CLBE (eV)	CLBES (eV)
O5	1	529.10	1.18
O3	1	529.28	1.36
O1*	1	530.95	3.03
O5*	1	528.97	1.05
O6	2	528.96	1.04
O1	2	530.94	3.02
O1*	2	529.30	1.38
O5*	2	529.10	1.18

H_2O			
Atom	Site	CLBE (eV)	CLBES (eV)
O8	1	527.89	-0.03
O1	1	528.12	0.20
O5*	1	527.96	0.04
Oads	1	532.53	4.61
O5	3	528.30	0.38
O1	3	527.83	-0.09
O1*	3	527.77	-0.15
Oads	3	532.97	5.05

O			
Atom	Site	CLBE (eV)	CLBES (eV)
O5	1	529.32	1.40
O1	1	527.55	-0.37
O5*	1	529.32	1.40
Oads	1	528.17	0.25
O7	2	529.32	1.40
O1*	2	527.50	-0.42
O5*	2	529.33	1.41
Oads	2	528.16	0.24

CO_2			
Atom	Site	CLBE (eV)	CLBES (eV)
O8	1	531.20	3.28
O1*	1	528.80	0.88
O5*	1	529.41	1.49
Oads_1	1	530.89	2.97
Oads_2	1	530.60	2.68
O1	2	528.17	0.25
O1*	2	527.85	-0.07
O5*	2	530.57	2.65
Oads_1	2	530.21	2.29
Oads_2	2	530.13	2.21

OH			
Atom	Site	CLBE (eV)	CLBES (eV)
O1	1	528.69	0.77
O1*	1	527.98	0.06
O5*	1	528.42	0.50
Oads	1	529.46	1.54
O1	2	528.63	0.71
O1*	2	528.04	0.12
O5*	2	528.26	0.34
Oads	2	529.42	1.50

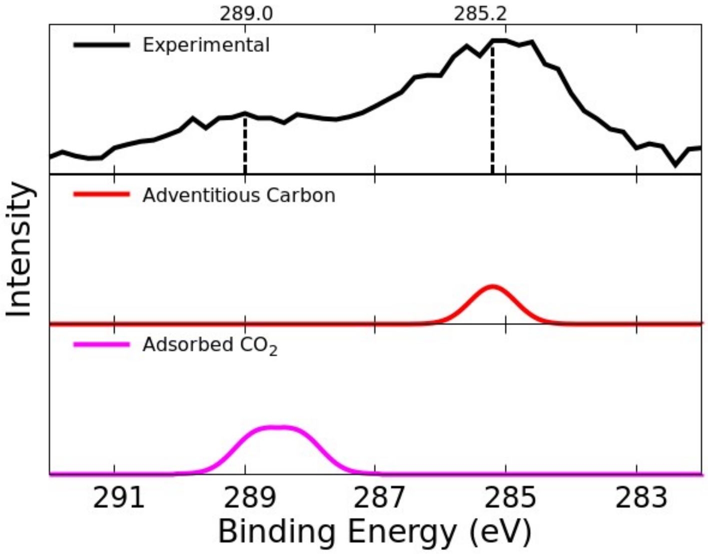

Figure S21: Experimental XPS C 1*s* $LaCoO_3$ surface data plotted with two peaks one at 285.2 eV and one at 289.0 eV.

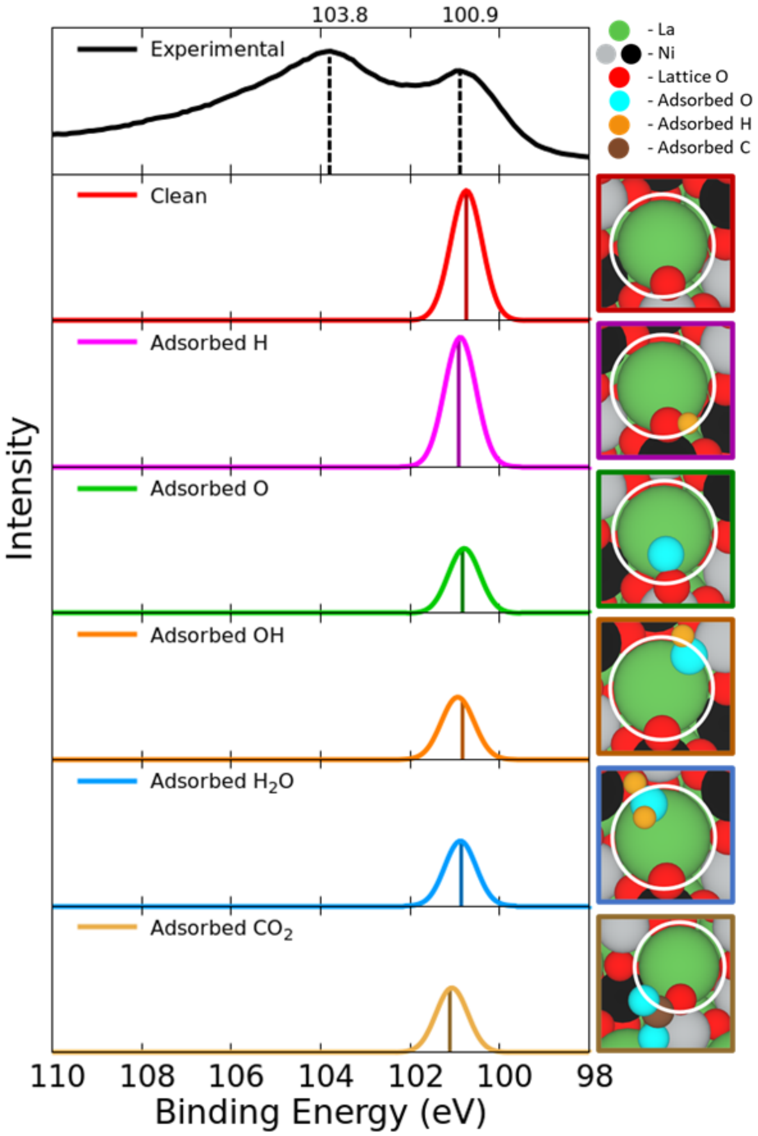

Figure S22: Experimental XPS La 4*d* for $LaNiO_3$ surface data plotted with two peaks one at 100.9 eV and one at 103.8 eV. The second graph depicts the spectra of the surface without adsorbed species and last four graphs show the effects of the adsorbed species on the nearby surface atoms. On the right: Images of species contributing to each of the peaks in the presence of adsorbed atoms/molecules. The border color corresponds to the energies marked on the theoretical XPS graph. Spin up and spin down Ni are shown in black and grey respectively. The corresponding atoms are circled in white.

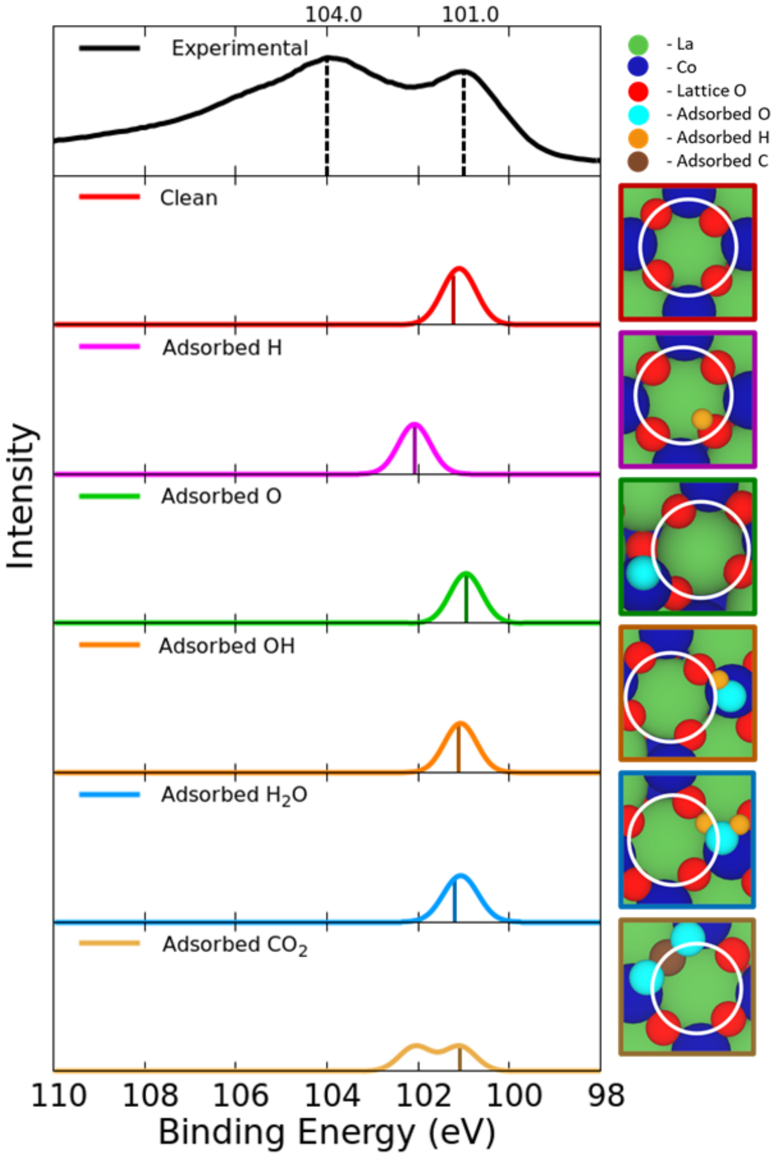

Figure S23: Experimental XPS La 4*d* for $LaCoO_3$ surface data plotted with two peaks one at 101.0 eV and one at 104.0 eV. The second graph depicts the spectra of the surface without adsorbed species and last four graphs show the effects of the adsorbed species on the nearby surface atoms. On the right: Images of species contributing to each of the peaks in the presence of adsorbed atoms/molecules. The border color corresponds to the energies marked on the theoretical XPS graph.

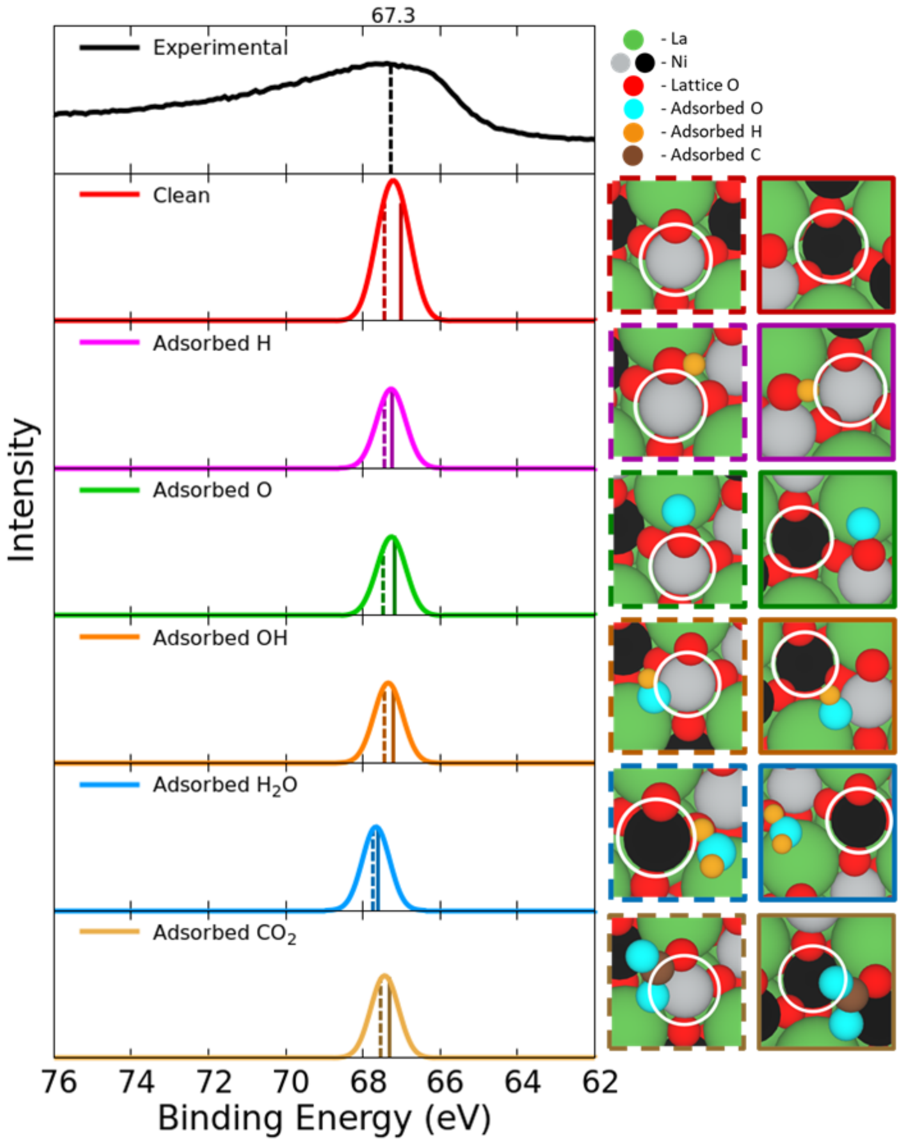

Figure S24: Experimental XPS Ni 3*p* for $LaNiO_3$ surface data plotted with one peak at 67.3 eV. The second graph depicts the spectra of the surface without adsorbed species and last four graphs show the effects of the adsorbed species on the nearby surface atoms. On the right: Images of species contributing to each of the peaks in the presence of adsorbed atoms/molecules. The border color corresponds to the energies marked on the theoretical XPS graph. Spin up and spin down Ni are shown in black and grey respectively. The corresponding atoms for which the spectra are simulated are circled in white.

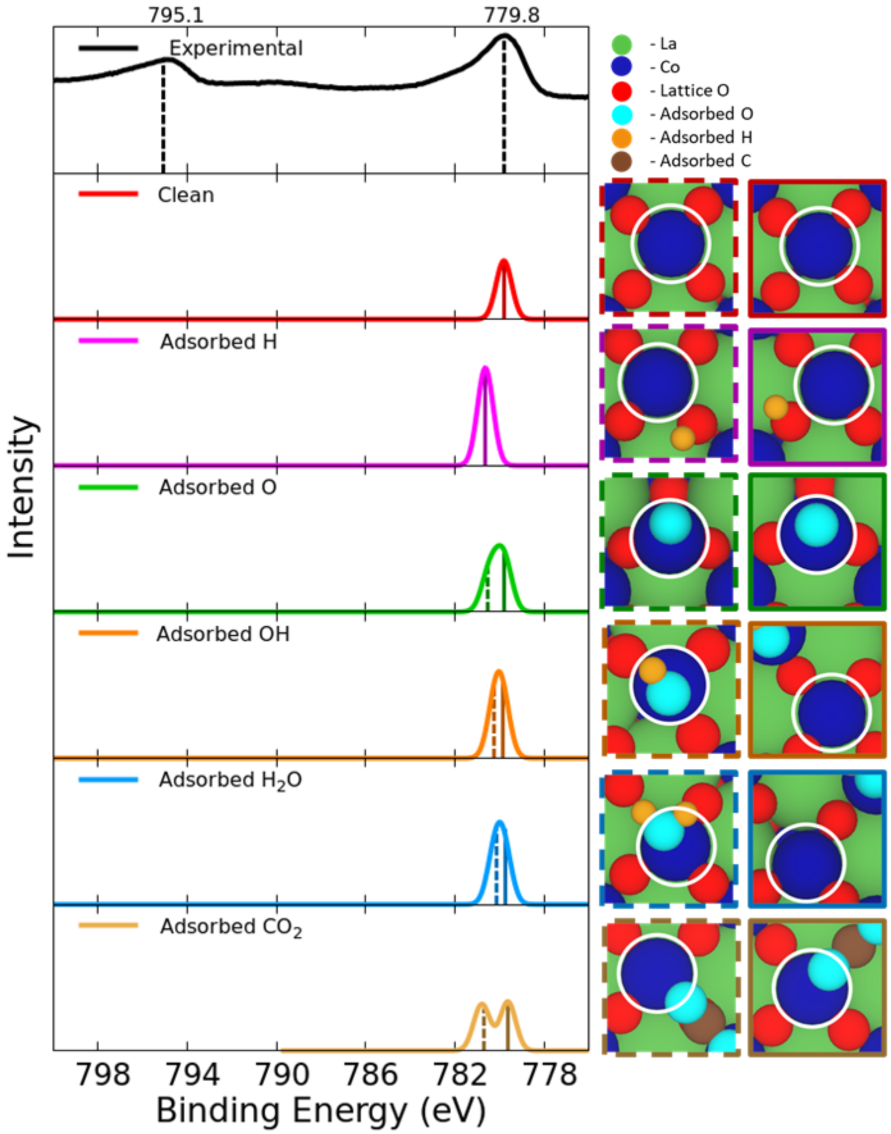

Figure S25: Experimental XPS Co 2*p* for $LaCoO_3$ surface data plotted with two peaks one at 795.1 eV and one at 779.8 eV. The second graph depicts the spectra of the surface without adsorbed species and last four graphs show the effects of the adsorbed species on the nearby surface atoms. On the right: Images of species contributing to each of the peaks in the presence of adsorbed atoms/molecules. The border color corresponds to the energies marked on the theoretical XPS graph.

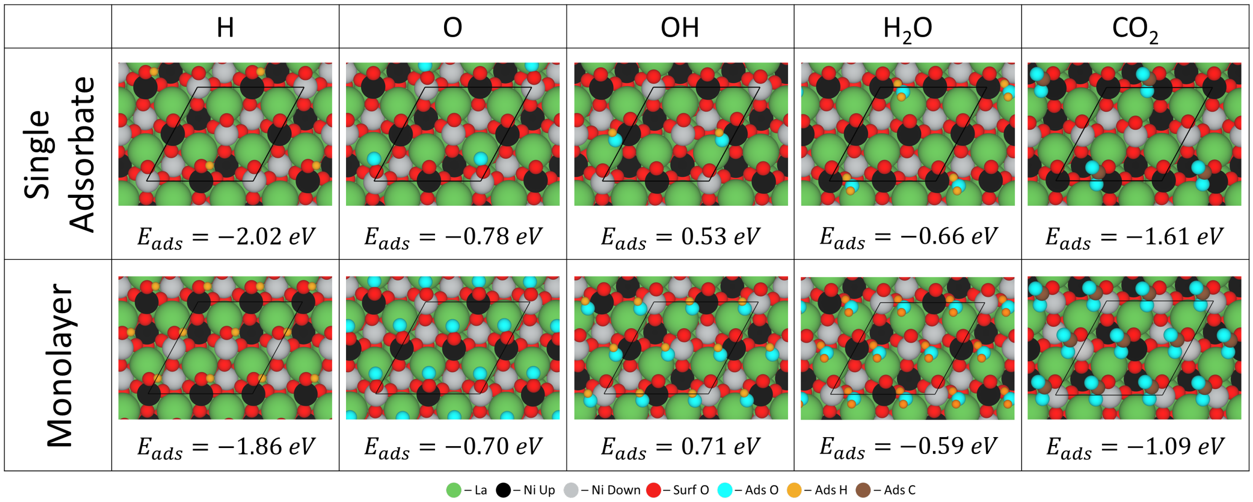

Figure S26: A comparison between adsorbate adsorption energies with a single adsorbate on the surface or a monolayer coverage $LaNiO_3$. The case for each adsorbate was chosen as the most favorable adsorption position when adsorbed in a single adsorbate case.

Table S10: CLBESs contributions to each theoretical spectra shown in Figures S27-S31 for monolayer adsorption on $LaNiO_3$. These values have been convoluted using Gaussians to create theoretical spectra.

H		
Atom	CLBE (eV)	CLBES (eV)
O1	530.24	2.99
O2	530.15	2.90
O3	530.16	2.91
O4	530.18	2.93
O5	528.12	0.87
O8	528.13	0.88
O11	528.50	1.25
O12	528.52	1.27
O15	528.50	1.25
O18	528.36	1.11
O23	528.42	1.17

H_2O		
Atom	CLBE (eV)	CLBES (eV)
O1	527.48	0.23
O2	527.49	0.24
O5	528.15	0.90
O8	528.14	0.89
O12	528.49	1.24
O14	528.44	1.19
O15	528.47	1.22
Oads1	532.70	5.45
Oads2	532.40	5.15
Oads3	532.36	5.11
Oads4	532.34	5.09

O		
Atom	CLBE (eV)	CLBES (eV)
O1	530.37	3.12
O5	528.27	1.02
O8	528.32	1.07
O11	528.52	1.27
O12	528.46	1.21
O15	528.52	1.27
O18	528.25	1.00
Oads1	529.77	2.52
Oads2	529.79	2.54
Oads3	529.63	2.38
Oads4	529.85	2.60

CO_2		
Atom	CLBE (eV)	CLBES (eV)
O1	529.88	2.63
O2	529.98	2.73
O5	528.42	1.17
O10	528.27	1.02
O12	528.42	1.17
O14	528.21	0.96
O23	528.21	0.96
Oads1	530.36	3.11
Oads2	529.89	2.64
Oads3	530.00	2.75
Oads4	530.15	2.90
Oads5	529.48	2.23
Oads6	529.29	2.04
Oads7	529.47	2.22
Oads8	529.61	2.36

OH		
Atom	CLBE (eV)	CLBES (eV)
O1	527.08	-0.17
O2	527.02	-0.23
O5	527.80	0.55
O10	527.98	0.73
O12	528.08	0.83
O14	528.21	0.96
O18	528.17	0.92
Oads1	529.14	1.89
Oads2	529.18	1.93
Oads3	529.13	1.88
Oads4	529.15	1.90

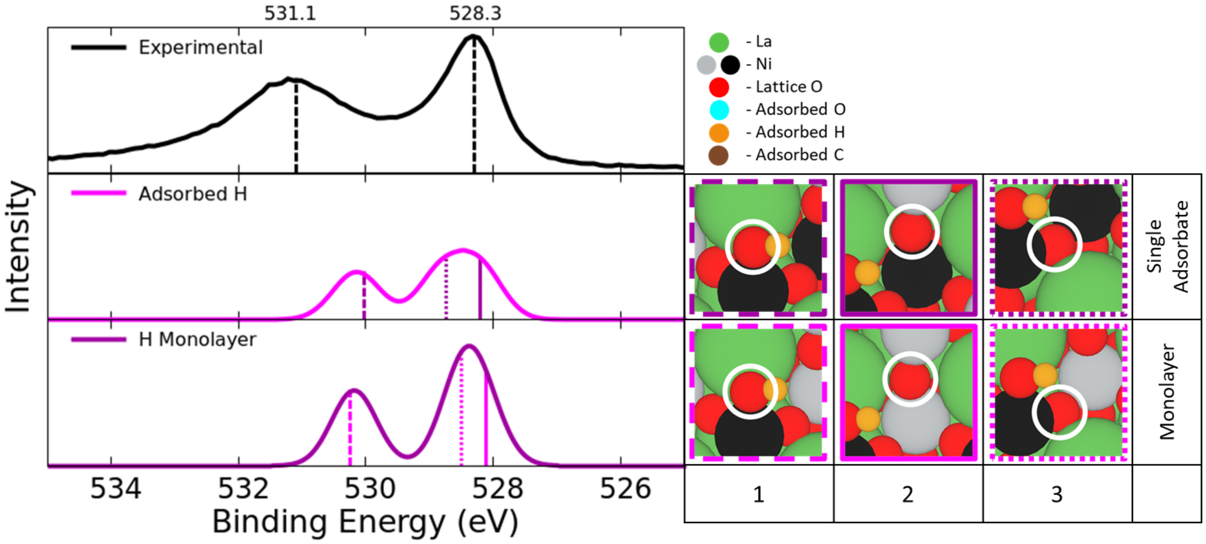

Figure S27: Experimental XPS O 1*s* for $LaNiO_3$ surface data plotted with two peaks one at 531.1 eV and one at 528.3 eV. Below the experimental spectra there is a single adsorbate and monolayer case for H. On the right: Images of species contributing to each of the peaks in the presence of adsorbed atoms/molecules. The border color and line type correspond to the energies marked on the theoretical XPS graph. Spin up and spin down Ni are shown in black and grey respectively. The corresponding O species for which the XPS is simulated are circled in white.

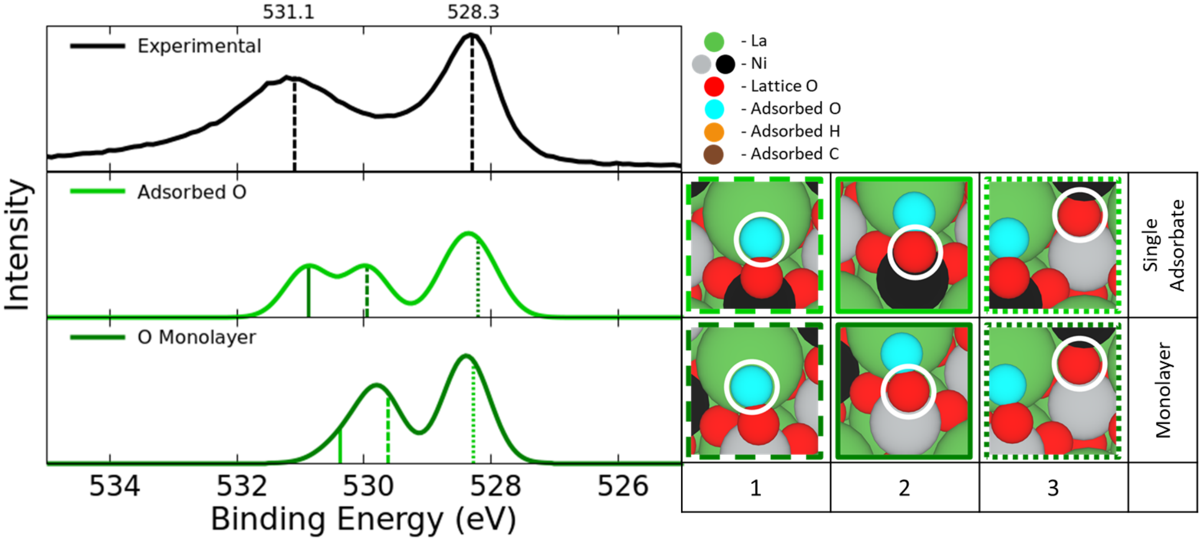

Figure S28: Experimental XPS O 1*s* for $LaNiO_3$ surface data plotted with two peaks one at 531.1 eV and one at 528.3 eV. Below the experimental spectra there is a single adsorbate and monolayer case for O. On the right: Images of species contributing to each of the peaks in the presence of adsorbed atoms/molecules. The border color and line type correspond to the energies marked on the theoretical XPS graph. Spin up and spin down Ni are shown in black and grey respectively. The corresponding O species for which the XPS is simulated are circled in white.

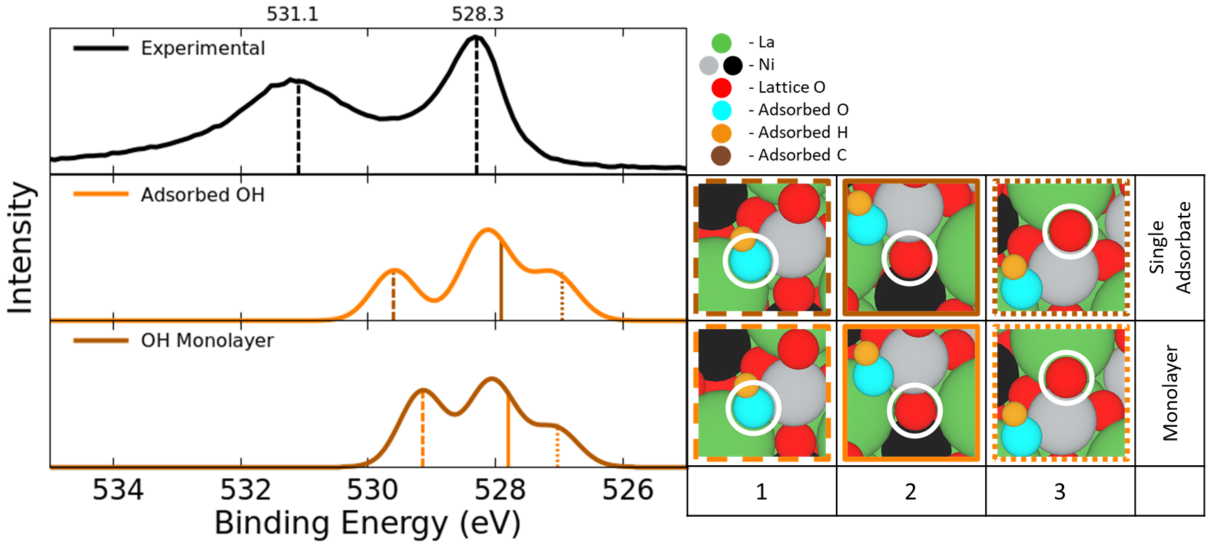

Figure S29: Experimental XPS O 1*s* for $LaNiO_3$ surface data plotted with two peaks one at 531.1 eV and one at 528.3 eV. Below the experimental spectra there is a single adsorbate and monolayer case for OH. On the right: Images of species contributing to each of the peaks in the presence of adsorbed atoms/molecules. The border color and line type correspond to the energies marked on the theoretical XPS graph. Spin up and spin down Ni are shown in black and grey respectively. The corresponding O species for which the XPS is simulated are circled in white.

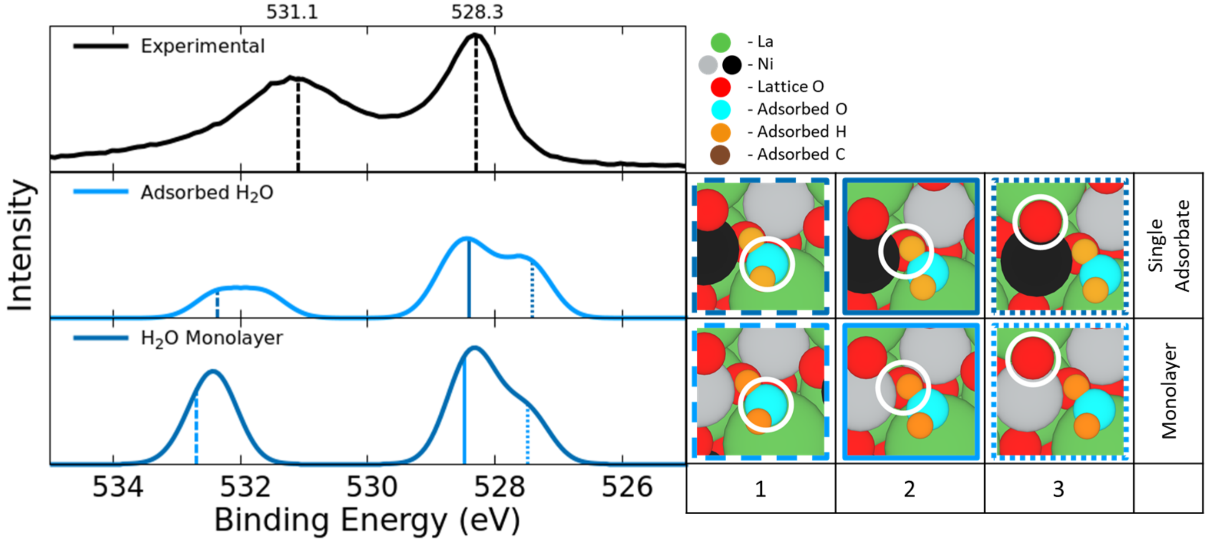

Figure S30: Experimental XPS O 1*s* for $LaNiO_3$ surface data plotted with two peaks one at 531.1 eV and one at 528.3 eV. Below the experimental spectra there is a single adsorbate and monolayer case for H_2O. On the right: Images of species contributing to each of the peaks in the presence of adsorbed atoms/molecules. The border color and line type correspond to the energies marked on the theoretical XPS graph. Spin up and spin down Ni are shown in black and grey respectively. The corresponding O species for which the XPS is simulated are circled in white.

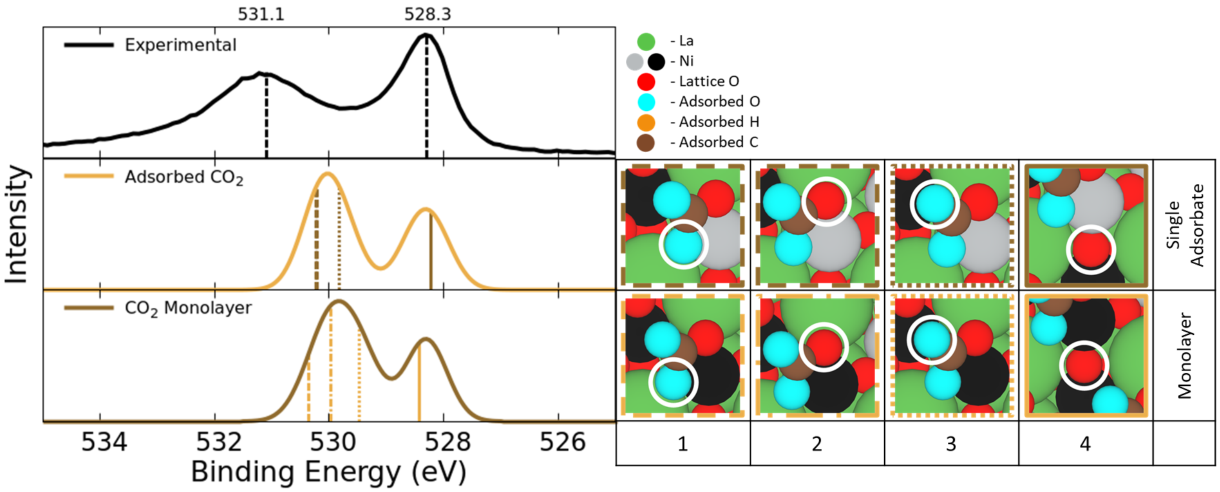

Figure S31: Experimental XPS O 1*s* for $LaNiO_3$ surface data plotted with two peaks one at 531.1 eV and one at 528.3 eV. Below the experimental spectra there is a single adsorbate and monolayer case for CO_2. On the right: Images of species contributing to each of the peaks in the presence of adsorbed atoms/molecules. The border color and line type correspond to the energies marked on the theoretical XPS graph. Spin up and spin down Ni are shown in black and grey respectively. The corresponding O species for which the XPS is simulated are circled in white.

Table S11: Differences between the CLBESs of a single adsorbate on the surface vs. a monolayer coverage.

H			
Atom	SA CLBES (eV)	ML CLBES (eV)	Difference
1	2.78	2.99	0.21
2	0.96	0.87	-0.09
3	1.48	1.25	-0.23

H_2O			
Atom	SA CLBES (eV)	ML CLBES (eV)	Difference
1	5.11	5.45	0.34
2	1.16	1.24	0.08
3	0.17	0.24	0.07

O			
Atom	SA CLBES (eV)	ML CLBES (eV)	Difference
1	2.7	2.38	-0.32
2	3.63	3.12	-0.51
3	0.96	1.02	0.06

CO_2			
Atom	SA CLBES (eV)	ML CLBES (eV)	Difference
1	2.96	3.11	0.15
2	2.98	2.73	-0.25
3	2.58	2.23	-0.35
4	0.97	1.17	0.2

OH			
Atom	SA CLBES (eV)	ML CLBES (eV)	Difference
1	2.36	1.9	-0.46
2	0.66	0.55	-0.11
3	-0.29	-0.23	0.06

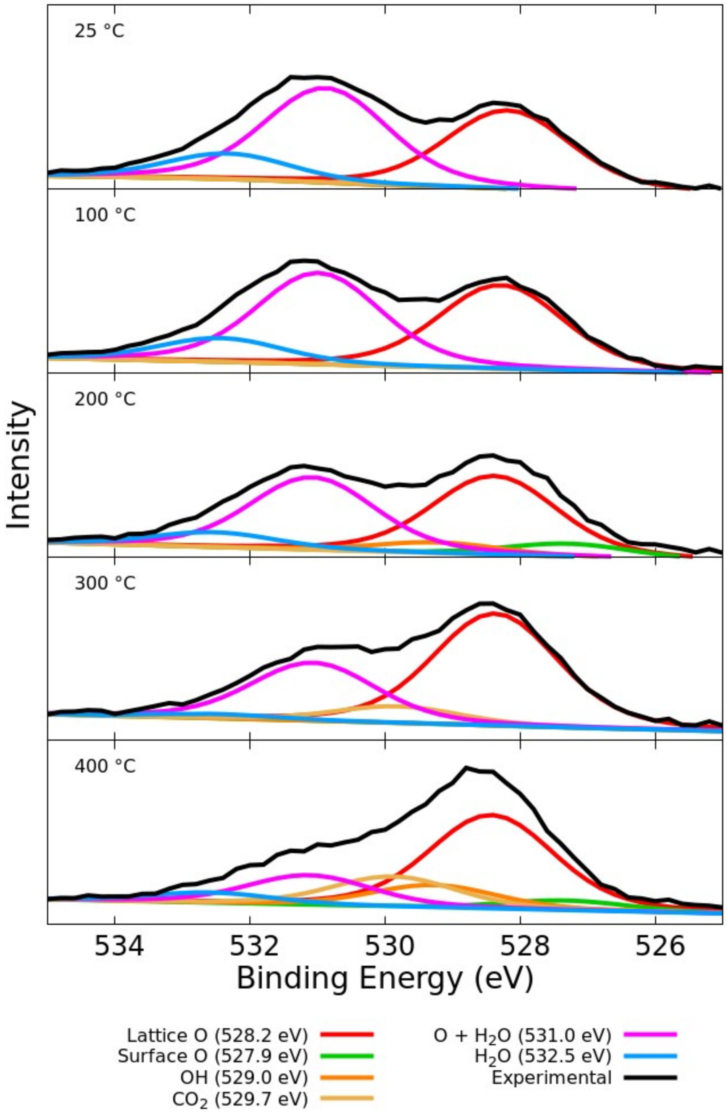

Figure S32: Experimental temperature-dependent O 1*s* spectra for LaNiO$_3$ with results for 25 °C, 100 °C, 200 °C 300 °C and 400 °C. The colored lines represent contributions determined by the theoretical spectra with both monolayer coverage and single adsorbates. The assignment shows the major adspecies represented by that particular contribution.

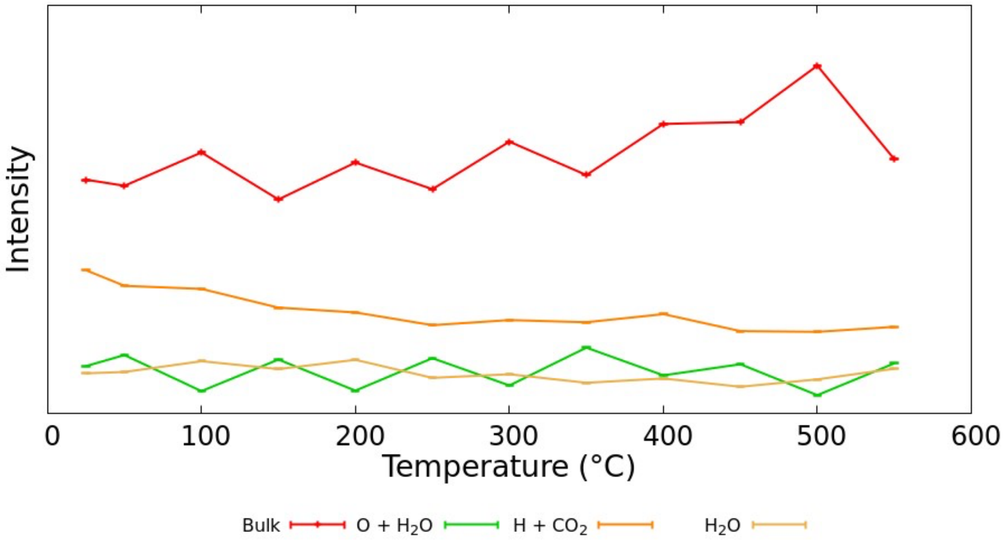

Figure S33: O 1*s* contributions to the experimental XPS spectra for $LaCoO_3$ as a function of temperature based on a similar analysis as for $LaNiO_3$.

References

(1) Tezel, E.; Guo, D.; Whitten, A.; Yarema, G.; Freire, M.; Denecke, R.; McEwen, J.-S.; Nikolla, E. Elucidating the Role of B-Site Cations Toward CO_2 Reduction in Perovskite-Based Solid Oxide Electrolysis Cells. *Journal of The Electrochemical Society* **2022**, *169* (3), 034532. DOI: 10.1149/1945-7111/ac5e9b.

(2) Kahk, J. M.; Lischner, J. Core Electron Binding Energies of Adsorbates on Cu(111) From First-Principles Calculations. *Physical Chemistry Chemical Physics* **2018**, *20* (48), 30403-30411. DOI: 10.1039/C8CP04955F.